

Original Article

BRCA1-associated protein 1 serves as a tumor suppressor in hepatocellular carcinoma by deubiquitinating and stabilizing PTEN

Xuxiao Chen^{1,2*}, Ao Huang^{2*}, Yupeng Wang², Feiyu Chen², Bo Hu², Xin Zhang², Yunfan Sun², Jian Wang², Jianwen Cheng^{2,3}, Pengxiang Wang², Yuan Ji^{4,5}, Shuangjian Qiu^{2,3}, Jia Fan^{2,3}, Jian Zhou^{2,3}, Xinrong Yang^{2,3}

¹Department of General Surgery, Hepatobiliary Surgery, Ruijin Hospital, Shanghai Jiao Tong University School of Medicine, Shanghai 200025, China; ²Department of Liver Surgery and Transplantation, Liver Cancer Institute, Zhongshan Hospital, Fudan University, Key Laboratory of Carcinogenesis and Cancer Invasion (Fudan University), Ministry of Education, Shanghai 200032, China; ³Shanghai Key Laboratory of Organ Transplantation, Zhongshan Hospital, Fudan University, Shanghai 200032, China; ⁴Department of Laboratory Medicine, Zhongshan Hospital, Fudan University, Shanghai 200032, China; ⁵Department of Pathology, Zhongshan Hospital, Fudan University, Shanghai 200032, China. *Equal contributors.

Received October 8, 2020; Accepted December 28, 2020; Epub May 15, 2021; Published May 30, 2021

Abstract: BRCA1-associated protein 1 (BAP1) or its mutants have been known to play critical regulatory roles in tumor biology, yet their role in hepatocellular carcinoma (HCC) remains largely unclear. In this study, we detected the mutations of all the exons of BAP1 in 105 HCC patients using Sanger sequencing, and found eight somatic mutations in 6 (5.71%) patients. We also found that the mRNA and protein levels of BAP1 were markedly downregulated in HCC versus the adjacent non-tumor tissues. Wild-type BAP1 but not mutant BAP1 significantly inhibited HCC cell proliferation, invasion, epithelial-mesenchymal transition (EMT) *in vitro*, and tumor progression and metastasis *in vivo*. Mechanistically, BAP1 complexed with PTEN and stabilized PTEN via deubiquitination and, furthermore, negatively regulated HCC cell EMT by deactivating the AKT/GSK-3 β /Snail pathway. However, those tumor-inhibitory effects of BAP1 were abolished by inactivating mutations. Clinically, low BAP1 expression was positively correlated to aggressive tumor phenotypes, which also independently associated with poorer recurrence-free survival and overall survival after curative hepatectomy. Conclusively, our results indicate that BAP1, significantly downregulated, somatically mutated and negatively regulating EMT in HCC, serves as a tumor suppressor of HCC by deubiquitinating and stabilizing PTEN.

Keywords: Hepatocellular carcinoma, BAP1, tumor suppressor, PTEN, prognosis

Introduction

The incidence and mortality of hepatocellular carcinoma (HCC) has kept increasing in recent years, making HCC as one of the most lethal cancer worldwide [1, 2]. Currently, liver transplantation or hepatectomy is the main standard curative therapy for patients with HCC, but the long-term prognosis after these treatments remains dissatisfactory because of frequent recurrence and metastasis [3, 4]. Still worse, the development of molecular targeted therapies or chemotherapies is obstructed by the poor understanding of HCC pathogenesis. Therefore, exploring the molecular mecha-

nisms underlying HCC progression and metastasis is critical for identifying new effective therapeutic targets.

BRCA1-associated protein 1 (BAP1) belongs to the deubiquitinating enzyme (DUB) superfamily, which is homologous to other ubiquitin carboxyl-terminal hydrolase (UCH) containing a N-terminal catalytic domain [5]. BAP1 locates at chromosome 3p21, which is a hotspot that frequently mutates in human cancer [5, 6]. Loss of BAP1 expression or inactivating genetic variants in the BAP1 gene locus have been found in various malignancies [5, 7-16]. The germline or somatic mutations in BAP1 gene

BAP1 suppresses HCC invasion by deubiquitinating PTEN

often lead to reduced expression or loss of protein function, which then accelerates tumor initiation, progression, and metastasis [9, 14, 16]. Importantly, recurrent somatic mutations of BAP1 have been found in HCC, and some of which located on the deubiquitinase region, which is vital to its deubiquitinating activity [17, 18]. Therefore, it is possible that BAP1 deficiency may play a crucial role in HCC progression and metastasis.

In the present study, we identified that BAP1 harbored somatic mutations in HCC. BAP1 was markedly downregulated in HCC, and its deficiency was correlated to aggressive tumor phenotypes and poor postoperative prognosis. Further functional experiments indicated that BAP1 suppressed HCC cell proliferation, invasion, epithelial-mesenchymal transition (EMT) *in vitro* and tumor progression and metastasis *in vivo*, by forming a complex with phosphatase and tensin homolog (PTEN) and stabilizing PTEN via deubiquitination. We further demonstrated that those tumor-inhibitory effects of BAP1 were abolished by inactivating mutations. Therefore, BAP1 serves as a tumor suppressor of HCC, which provides a potential candidate treatment target in HCC.

Materials and methods

HCC samples and follow-up

Human liver tissues were collected from HCC patients that underwent curative hepatectomy at the Liver Cancer Institute, Zhongshan Hospital, Fudan University (Shanghai, China). The study was granted approval from the research ethics committee of Zhongshan Hospital, and each patient in this study provided informed consent.

Paired snap-frozen tumor and adjacent non-tumor samples from 105 patients with HCC treated between March and July 2011 were consecutively collected for Sanger sequencing. Paired snap-frozen tumor and adjacent non-tumor samples from 66 patients with HCC treated between July and September 2011 were used for analyzing the expression of BAP1 messenger RNA (mRNA), while 12 pairs of which were randomly selected for evaluating the expression of BAP1 protein. Snap-frozen HCC samples from 12 patients without or with early tumor recurrence were used for analyzing the mRNA and protein expression of BAP1 to

assess the correlation with early recurrence. Paired paraffin-embedded HCC tissues and adjacent non-tumor tissues from 396 consecutive patients with HCC treated with curative hepatectomy between 2000 and 2002 were retrieved for constructing tissue microarray (TMA) and immunohistochemistry (IHC) analysis. Histopathological diagnosis was performed according to World Health Organization criteria. We classified tumor grade using the classification proposed by Edmondson and Steiner [19], and used the Chinese HCC staging system for tumor stage determination [2]. Clinical information collection and postoperative surveillance were conducted as previously described [20].

Recurrence-free survival (RFS) was the time from surgery to tumor recurrence. Overall survival (OS) was the duration from surgery to death. Data for patients alive were censored at the last follow-up.

Other materials and methods

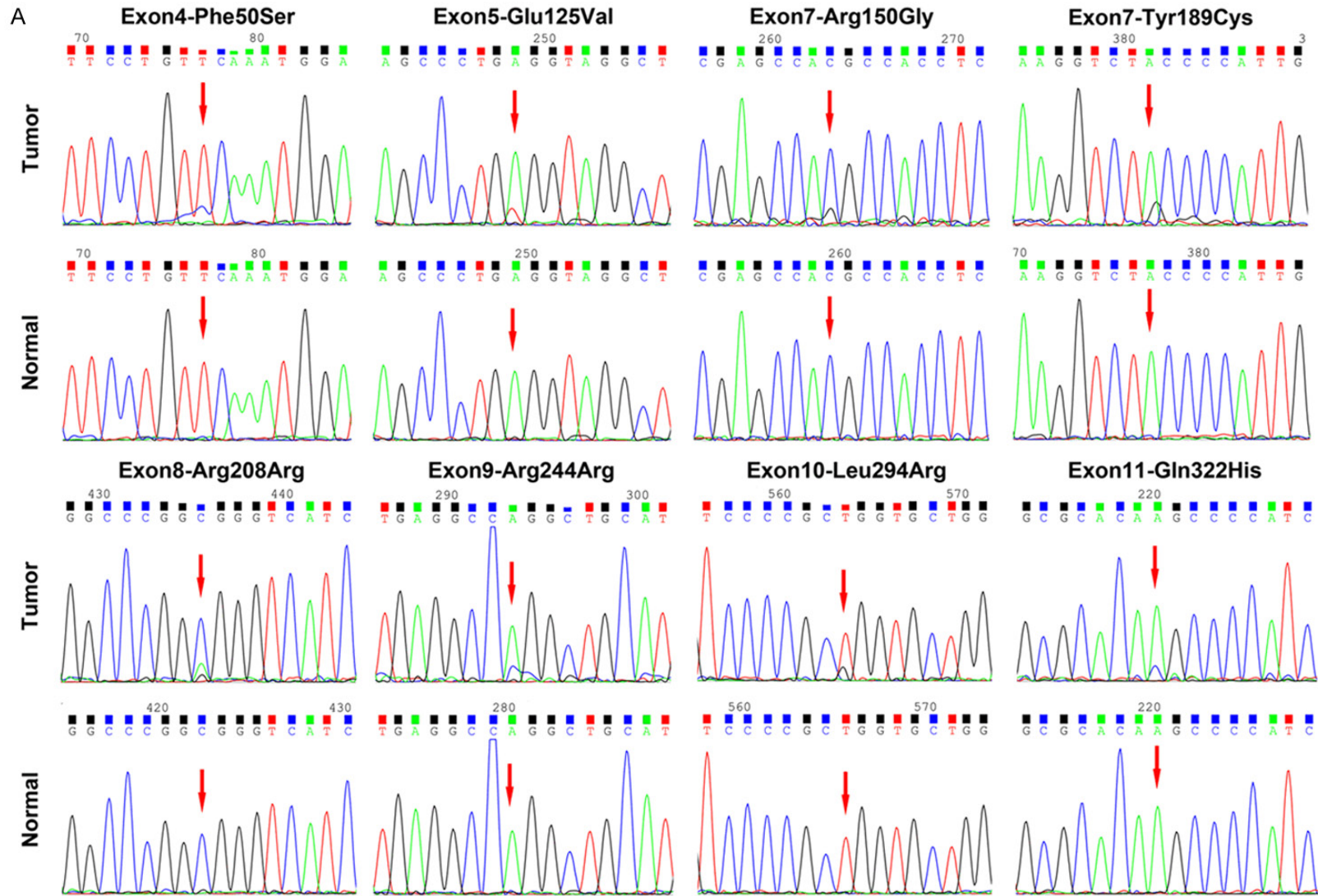
Details of TMA construction, IHC analysis, Sanger sequencing, protein structural/array analysis, sequence alignment analysis, cell lines and transfection, polymerase chain reaction (PCR), qRT-PCR, immunoprecipitation (IP), deubiquitination assay, western blot, immunofluorescence, functional *in vitro* and *in vivo* assays, and statistical analysis are described in the [Supplementary Materials and Methods](#). The sequences of mutant BAP1 variants, target sequences of short hairpin (sh) RNA, antibodies, and primer sequences used for Sanger sequencing are respectively listed in [Tables S1, S2, S3, S4](#).

Results

Prevalence screening of somatic BAP1 mutations in HCC

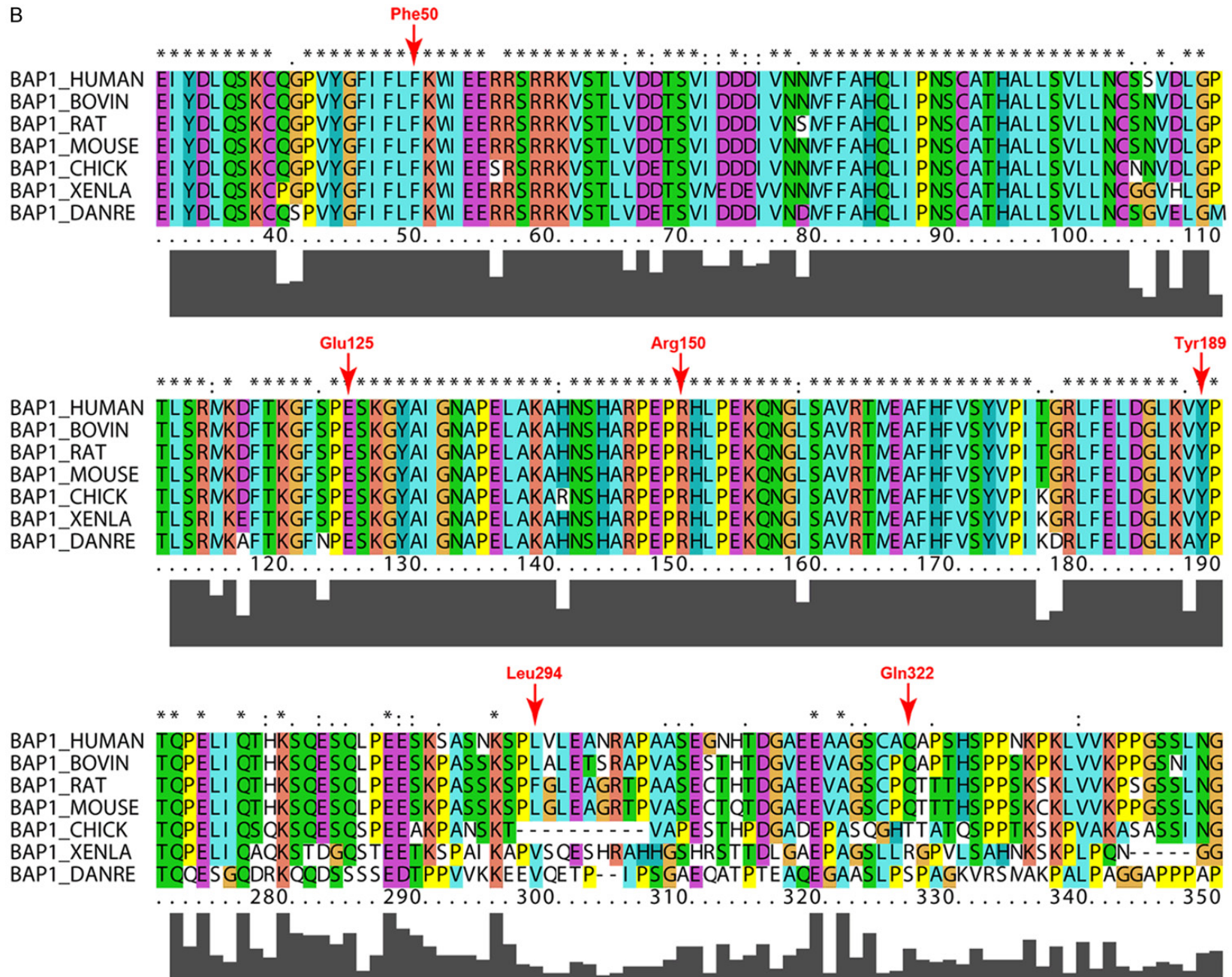
All the exons of BAP1 in 105 HCC patients were sequenced by Sanger sequencing, and eight somatic mutations were identified in six patients (6/105, 5.71%). Among the six HCCs containing somatic mutations in BAP1, two of which harbored two mutations each, and the others only had one single mutation each. The eight somatic mutations of BAP1 were located in exons 4, 5, 7, 8, 9, 10, and 11 of BAP1, and five of which were located in the UCH domain (**Figure 1A; Table 1**). According to Polyphen-2 analysis [21], four missense mutations located

BAP1 suppresses HCC invasion by deubiquitinating PTEN



BAP1 suppresses HCC invasion by deubiquitinating PTEN

B



BAP1 suppresses HCC invasion by deubiquitinating PTEN

Figure 1. Somatic mutations of BAP1 in HCC and multiple sequence alignments of BAP1 paralogs in different vertebrate species. A. Trace images of BAP1 mutations identified by Sanger sequencing in HCC. The sequenced regions of tumor tissues were compared with those of adjacent non-tumor tissues to confirm the somatic nature of these mutations. The red arrows indicated the mutation sites. B. Multiple sequence alignments of BAP1 paralogs in different vertebrate species, including human, bovine, rat, mouse, chicken, clawed frog, and zebrafish. The mutation sites in BAP1 were marked with red arrows.

Table 1. BAP1 mutations in 105 HCC samples

Exon No.	Nucleotide change (CDS)	Amino acid sequence change	Amino acid change	Mutation type	Polyphen-2 prediction (Score; Sensitivity; Specificity)	Case No.
4	c.T149C	TTC>TCC	p.Phe50Ser	Missense	PRD (1.000; 0.00; 1.00)	1
5	c.A374T	GAG>GTG	p.Glu125Val	Missense	PRD (1.000; 0.00; 1.00)	1
7	c.C448G	CGC>GGC	p.Arg150Gly	Missense	PRD (0.991; 0.71; 0.97)	1
7	c.A566G	TAC>TGC	p.Tyr189Cys	Missense	PRD (1.000; 0.00; 1.00)	1
8	c.C622A	CGG>AGG	p.Arg208Arg	Coding silent	-	1
9	c.A730C	AGG>CGG	p.Arg244Arg	Coding silent	-	1
10	c.T881G	CTG>CGG	p.Leu294Arg	Missense	Benign (0.148; 0.92; 0.86)	1
11	c.A966C	CAA>CAC	p.Gln322His	Missense	Benign (0.021; 0.95; 0.80)	1

Abbreviations: CDS, Coding sequence; PRD, probably damaging.

in the UCH domain (Phe50Ser, Glu125Val, Arg150Gly, and Tyr189Cys) were forecasted to adversely affect the function of BAP1 protein, whereas the other two missense mutations (Leu294Arg and Gln322His) were benign (**Table 1**). Furthermore, multiple species conservation analysis showed that the four residues mutated in the UCH domain (Phe50Ser, Glu125Val, Arg150Gly, and Tyr189Cys) affected the highly conserved regions of BAP1 (**Figure 1B**).

Structural and functional implications of BAP1 mutations

The mature BAP1 protein contains 729 amino acid residues, and all the somatic mutations of BAP1 identified in our study are located in the first half of BAP1 (**Figure 2A** and **2B**). According to the protein structure model, five mutations (Glu125Val, Arg150Gly, Tyr189Cys, Leu294Arg, and Gln322His) are located on the surface of BAP1 protein, which may play an important role in protein-protein interactions (**Figure 2C**). Based on the structural analysis (**Figure 2D**), we identified that four mutations (Phe50Ser, Glu125Val, Arg150Gly, and Gln322His) dramatically change the physicochemical characteristics of BAP1 such as hydrophobic residues to polar or acid residues etc. and the other two mutations (Tyr189Cys and Leu294Arg) also play important roles on the surface of BAP1. Combined with the results of the Polyphen-2 analysis and multiple species conservation

analysis, we speculate that the four missense mutations located in the UCH domain (Phe50Ser, Glu125Val, Arg150Gly, and Tyr189Cys) have implied structural and functional significance, which may inactivate BAP1 by impacting its deubiquitinase activity, structure stability, or substrate binding ability.

Clinical implications of BAP1 mutations in HCC

The clinical implications of somatic BAP1 mutations were investigated in the 105 HCC patients. We found that those somatic BAP1 mutations were more inclined to happen in HCC patients who had high level of AFP (5/58, 8.6%), tumor size >5 cm (4/42, 9.5%), multiple tumors (2/14, 14.3%), poor tumor differentiation (3/33, 9.1%), presence of vascular invasion (5/35, 14.3%), and presence of tumor recurrence (4/56, 7.1%). Additionally, the correlation analysis showed that these mutations were significantly correlated to vascular invasion ($P = 0.015$), but not with other clinicopathological characteristics ($P > 0.05$) (**Table S5**).

BAP1 was downregulated in human HCC

Given that BAP1 is somatically mutated in HCC, we then evaluated the expression of BAP1 in HCC, to further explore the functional role of BAP1 in HCC. We found that the mRNA expression of BAP1 was significantly reduced in 74.2% (49/66) of HCC, versus the adjacent non-tumor

BAP1 suppresses HCC invasion by deubiquitinating PTEN

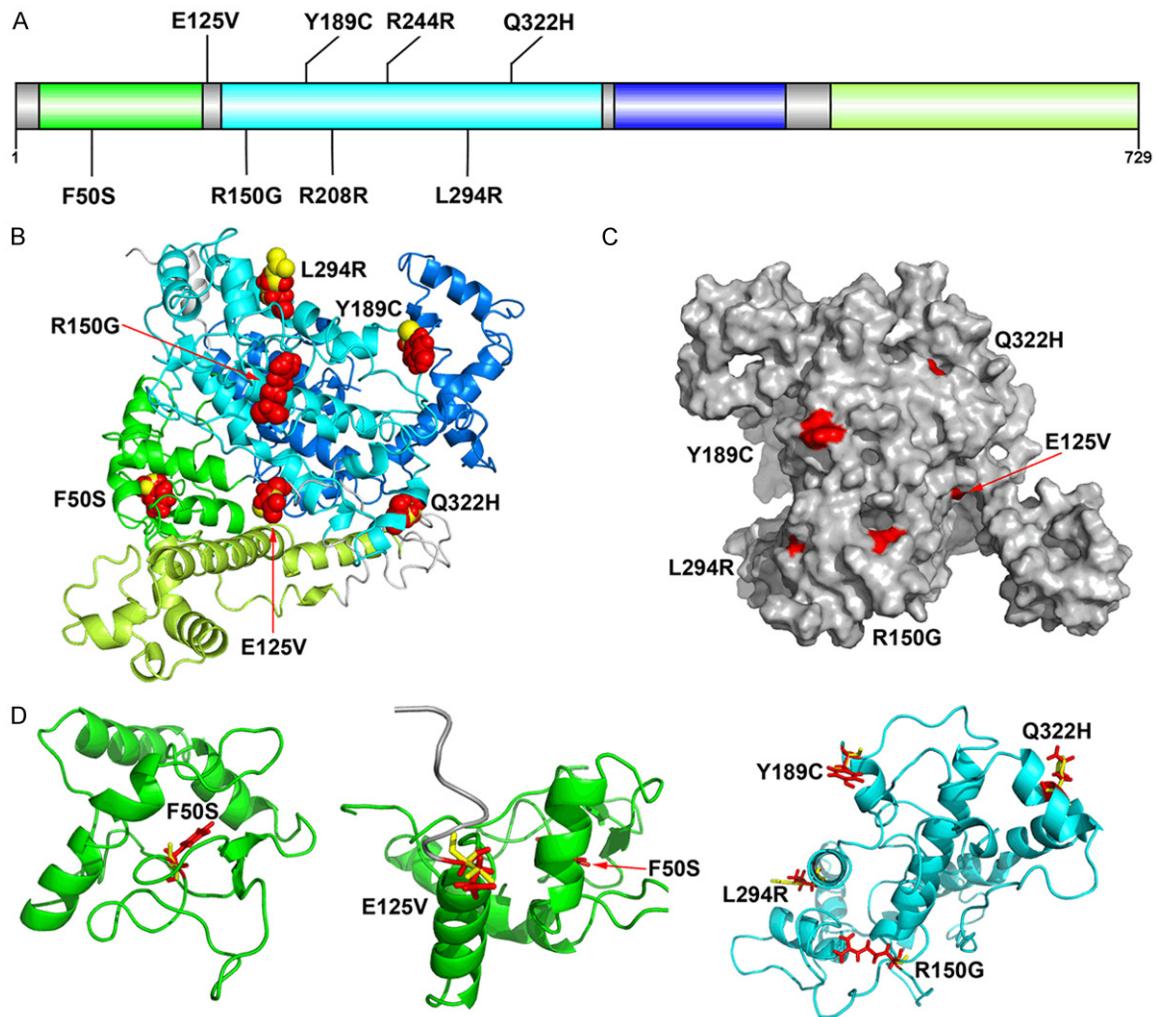


Figure 2. Schematic representation of the somatic BAP1 mutations in HCC. A. Distribution of the somatic BAP1 mutations in HCC. B. The full-length three-dimensional model of BAP1 protein and BAP1 missense mutations. The wild and mutated residues were shown in red and yellow spheres, respectively. C. Surface view of BAP1 protein and BAP1 missense mutations. The mutation residues were shown in red. D. A detailed view of the mutation residues F50S, E125V, and the other 4 residues (R150G, Y189C, L294R, and Q322H), respectively. The wild and mutated residues were shown in red and yellow sticks, respectively.

tissues ($P = 0.032$) (Figure 3A). Western blot assays showed similar results (Figure 3B). Next, IHC staining of BAP1 was performed in TMAs containing a cohort of 396 HCC patients. Low BAP1 expression (scored as negative or weak) was observed in 46.2% of tumor tissues (183/396) but only 27.2% of corresponding adjacent non-tumor liver tissues (108/396) (Figure 3C). Further, we examined the mRNA expression of BAP1 in the 105 HCC tissues that had been sequenced by Sanger sequencing to investigate the pertinence of mutation and expression of BAP1 in HCC. The results revealed that the mRNA expression level was comparable in HCC tissues without or with BAP1 mutations ($P = 0.386$), indicating that the mRNA

expression of BAP1 was independent of its mutation status (Figure S1). Moreover, to assess the correlation of BAP1 expression with early tumor recurrence, we further analyzed the mRNA and protein expression of BAP1 in 12 HCC samples and found that the expression of BAP1 in patients with tumor recurrence were much lower than in those without tumor recurrence (Figure 3D).

Clinical significance of BAP1 protein expression in HCC

In order to explore the clinical relevance of BAP1 in HCC, we dichotomized the 396 patients with HCC as BAP1^{high} group (scored strong or

BAP1 suppresses HCC invasion by deubiquitinating PTEN

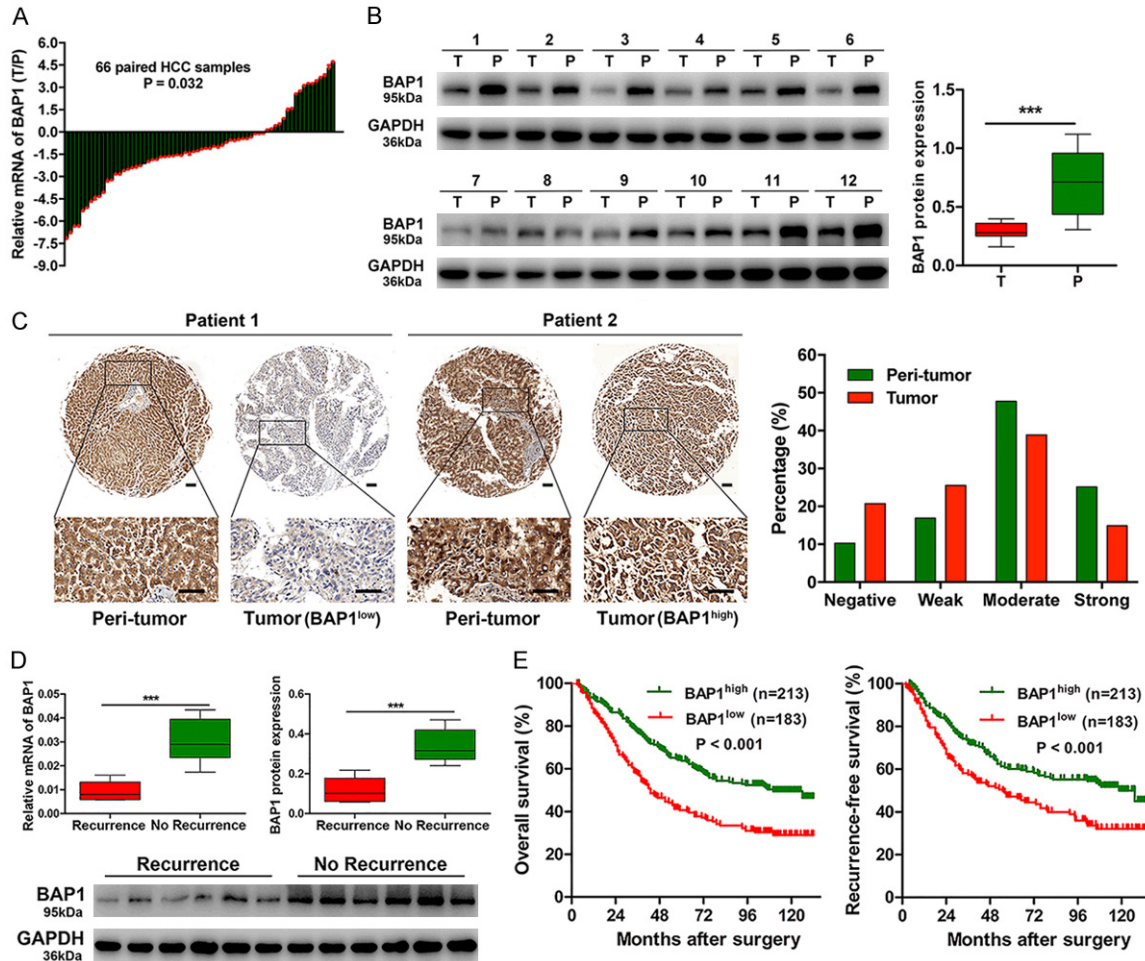


Figure 3. BAP1 was downregulated in HCC and correlated to poor postoperative survival. A. The expression level of BAP1 mRNA in paired tumor (T) and adjacent non-tumor samples (P) from 66 patients with HCC. B. The expression level of BAP1 protein in paired tumor (T) and adjacent non-tumor samples (P) from 12 patients with HCC. The protein level of BAP1 was expressed relative to GAPDH in the densitometry analysis. C. Representative IHC images of BAP1 protein in HCC tumor and matched adjacent non-tumor samples. The statistics of the score of BAP1 staining intensity in TMA was shown in the bar graph. Scale bars = 50 μ m. D. The expression levels of BAP1 mRNA and protein in HCC tissues without and with tumor recurrence after curative hepatectomy. E. Kaplan-Meier curves for OS and RFS in HCC patients based on BAP1 expression. Bar graphs described quantification of three independent results. *** $P < 0.001$.

moderate, $n = 213$) or BAP1^{low} group (scored weak or negative, $n = 183$). By analyzing the relationship of BAP1 expression and clinicopathological characteristics, we identified that low BAP1 expression was positively correlated to aggressive tumor phenotypes, such as greater tumor number ($P = 0.044$), larger tumor size ($P = 0.007$), appearance of vascular invasion ($P = 0.012$), and higher Chinese HCC stage ($P = 0.002$) (Table 2). Notably, the RFS and OS of patients with low BAP1 expression were significantly poorer compared with patients with high BAP1 expression, respectively ($P < 0.001$ and $P < 0.001$) (Figure 3E). The median RFS and OS were 55.0 months and 43.0 months for pa-

tients in BAP1^{low} group as compared with 118.5 months and 110.0 months for patients in BAP1^{high} group, respectively. Importantly, multivariate Cox analysis, which incorporated all significant variables identified by univariate analysis, revealed that low BAP1 expression was an independent predictor for RFS and OS (Table 3).

BAP1 deficiency promoted HCC progression and metastasis

We examined the expression of BAP1 in seven HCC cell lines. MHCC97L, MHCC97H and HCCLM3 cell lines showed low BAP1 expres-

BAP1 suppresses HCC invasion by deubiquitinating PTEN

Table 2. Correlation between BAP1 expression and clinicopathological characteristics in 396 HCC patients

Clinicopathological indexes		BAP1		P
		Low	High	
Age (year)	≤50	89	111	0.490
	>50	94	102	
Sex	Female	28	22	0.138
	Male	155	191	
HBsAg	Negative	32	39	0.831
	Positive	151	174	
HCV	Negative	179	207	0.758*
	Positive	4	6	
AFP (ng/ml)	≤20	68	73	0.550
	>20	115	140	
ALT (U/l)	≤75	167	192	0.704
	>75	16	21	
Liver cirrhosis	No	35	39	0.836
	Yes	148	174	
Tumor size (cm)	≤5	93	137	0.007
	>5	90	76	
Tumor number	Single	138	178	0.044
	Multiple	45	35	
Satellite	No	162	198	0.126
	Yes	21	15	
Tumor encapsulation	Complete	101	131	0.204
	None	82	82	
Vascular invasion	No	127	171	0.012
	Yes	56	42	
Tumor differentiation	I-II	121	139	0.857
	III-IV	62	74	
Chinese HCC Stage	I	104	153	0.002
	II+IIIa	79	60	

Abbreviations: AFP, alpha-fetoprotein; ALT, alanine aminotransferase. *Fisher's exact tests, and χ^2 tests for all the other analysis.

sion, while relatively high BAP1 expression was observed in SMMC7721, Huh7, HepG2, and Hep3B cell lines (Figure 4A). To investigate the function role of BAP1 in HCC, wild-type (WT) BAP1 and shBAP1 were transfected into HCCLM3 and HepG2 cell lines respectively, both of which were validated to be WT for BAP1. The transfection efficiency of these lentiviral vectors was validated using qRT-PCR, western blot, and immunofluorescence (Figures 4A, S2).

In the CCK8 proliferation, scratch and Matrigel invasion assays, overexpressing BAP1 in

HCCLM3 cells markedly inhibited cell viability, proliferation, migration and invasion, whereas downregulating BAP1 in HepG2 cells yielded an opposing effect (Figure 4B and 4C). Next, to validate the biological significance of BAP1 mutations, we generated plasmids encoding WT BAP1 or mutant BAP1 (Phe50Ser, Glu125Val, Arg150Gly, and Tyr189Cys), and then transfected them into HCCLM3 cells. As expected, overexpressing WT BAP1 in HCCLM3 cells notably inhibited cell proliferation. However, overexpressing mutant BAP1 in HCCLM3 cells did not yield a significant inhibiting effect. Moreover, HCCLM3 cells overexpressing mutant BAP1 displayed markedly increased proliferation, migration and invasion capability, versus HCCLM3 cells overexpressing WT BAP1 (Figure 4D-F). Evidently, those results indicated that BAP1 was a tumor suppressor of HCC and inactivated by its somatic mutations in HCC.

In the *in vivo* study, human HCC orthotopic transplantation model was established. The tumor size of xenografts originated from HepG2-shBAP1 and HCCLM3-Mock cells were $1.81 \pm 0.27 \text{ cm}^3$ and $2.33 \pm 0.43 \text{ cm}^3$, which were notably larger than that originated from HepG2-Mock and HCCLM3-BAP1 cells ($0.81 \pm 0.46 \text{ cm}^3$ and $1.18 \pm 0.52 \text{ cm}^3$, $P = 0.003$ and $P = 0.005$, respectively) (Figure 5A). Pulmonary metastasis of HCC occurred in 60% (3/5) of HepG2-shBAP1 mice and 100% (5/5) of HCCLM3-Mock mice, and the rates were significantly high than the rates of pulmonary metastasis in HepG2-Mock and HCCLM3-BAP1 mice (0% [0/5] and 20% [1/5], $P = 0.038$ and $P = 0.010$, respectively) (Figure 5B). Node number of pulmonary metastasis of each grade was huger in HepG2-shBAP1 and HCCLM3-Mock mice, as compared with HepG2-Mock and HCCLM3-BAP1 mice, respectively (Figure 5C).

BAP1 complexed with PTEN and stabilized PTEN via deubiquitination

The biological function role of DUBs in cancer primarily depends on their substrate proteins, which are always important factors in tumor initiation and progression [22]. Therefore, an online protein-protein interaction repository (BioGRID database) were searched, and we identified PTEN was one of the BAP1 binding proteins (Figure 6). PTEN is an important tumor suppressor in cancers, and its ubiquitination status is of great importance to its activity and

BAP1 suppresses HCC invasion by deubiquitinating PTEN

Table 3. Univariate and multivariate analyses of prognostic factors in 396 HCC patients

Variables	OS		RFS	
	HR (95% CI)	P	HR (95% CI)	P
<i>Univariate analysis</i>				
Age, year (>50 versus ≤50)	0.930 (0.719-1.204)	0.584	0.980 (0.735-1.306)	0.890
Sex (male versus female)	1.205 (0.796-1.825)	0.379	1.074 (0.688-1.675)	0.755
HBsAg (positive versus negative)	1.417 (0.989-2.031)	0.058	1.106 (0.763-1.605)	0.594
AFP, ng/mL (>20 versus ≤20)	1.606 (1.211-2.130)	0.001	1.149 (0.853-1.549)	0.361
ALT, U/L (>75 versus ≤75)	0.919 (0.581-1.454)	0.719	0.776 (0.457-1.316)	0.347
Liver cirrhosis (yes versus no)	1.662 (1.148-2.406)	0.007	2.041 (1.326-3.141)	0.001
Tumor size, cm (>5 versus ≤5)	1.460 (1.127-1.892)	0.004	0.920 (0.682-1.241)	0.584
Tumor number (multiple versus single)	2.115 (1.578-2.836)	0.000	1.969 (1.399-2.769)	0.000
Satellite (yes versus no)	1.651 (1.090-2.503)	0.018	1.210 (0.724-2.021)	0.467
Tumor encapsulation (none versus complete)	1.447 (1.116-1.875)	0.005	1.146 (0.854-1.536)	0.363
Vascular invasion (yes versus no)	1.792 (1.351-2.377)	0.000	1.618 (1.171-2.236)	0.004
Tumor differentiation (III-IV versus I-II)	1.086 (0.829-1.424)	0.550	0.915 (0.672-1.248)	0.576
Chinese HCC stage (II+IIIa versus I)	2.075 (1.597-2.696)	0.000	1.861 (1.385-2.502)	0.000
BAP1 (low versus high)	1.847 (1.424-2.396)	0.000	1.679 (1.257-2.242)	0.000
<i>Multivariate analysis</i>				
AFP, ng/mL (>20 versus ≤20)	1.561 (1.173-2.076)	0.002	NA	NA
Liver cirrhosis (yes versus no)	1.751 (1.203-2.550)	0.003	1.971 (1.281-3.033)	0.002
Tumor size, cm (>5 versus ≤5)	1.401 (1.073-1.829)	0.013	NA	NA
Chinese HCC stage (II+IIIa versus I)	1.726 (1.320-2.257)	0.000	1.741 (1.293-2.343)	0.000
BAP1 (low versus high)	1.745 (1.340-2.272)	0.000	1.573 (1.177-2.103)	0.002

Cox proportional hazards regression model. Variables for multivariate analyses were adopted for their prognostic significance by univariate analysis ($P < 0.05$), and these variables were assessed for prognostic significance by univariate analysis with forward stepwise selection (forward, likelihood ratio). Abbreviations: 95% CI, 95% confidence interval; AFP, alpha-fetoprotein; ALT, Alanine aminotransferase; HR, Hazard Ratio; NA, not applicable.

expression [23]. Therefore, we sought to determine whether BAP1 can complex with PTEN and stabilize PTEN through deubiquitination.

To examine BAP1 complexing with PTEN, co-IP assays were performed in HepG2 cells. The results confirmed that endogenous BAP1 formed a complex with endogenous PTEN in HepG2 cells (**Figure 7A**). Several ubiquitin ligases have been reported to ubiquitinate PTEN protein, such as WWP2, CHIP, and TRIM27, etc. [24-26]. In order to investigate whether BAP1 could block the degradation of PTEN induced by ubiquitin ligases, PTEN, WWP2, or BAP1 were transfected into HCCLM3 cells and PTEN protein level was detected in indicated cells. Interestingly, WWP2 overexpression downregulated PTEN protein level, while BAP1 overexpression antagonized the degradation of PTEN mediated by WWP2 (**Figure 7B**).

To explore whether BAP1 can deubiquitinate PTEN, we transfected PTEN, Ub, WT BAP1 or

inactivating mutant BAP1 (Phe50Ser, Glu125Val, Arg150Gly, and Tyr189Cys) into HCCLM3 cells. The degradation of cell protein was blocked by treating indicated cells using MG132 (a proteasome inhibitor). Then, we tested polyubiquitinated PTEN proteins by western blot using anti-Ub antibody. The results showed that WT BAP1, instead of inactivating mutant BAP1 significantly decreased PTEN protein polyubiquitination (**Figure 7C**). By contrast, knockdown of endogenous BAP1 significantly increased endogenous PTEN protein polyubiquitination in HepG2 cells (**Figure 7C**). To further investigate whether BAP1 could stabilize PTEN against degradation, we overexpressed WT BAP1 or inactivating mutant BAP1 (Phe50Ser, Glu125Val, Arg150Gly, and Tyr189Cys) into HCCLM3 cells. The protein translation was blocked by treating indicated cells using cycloheximide (CHX, a protein synthesis inhibitor). Evidently, overexpression of WT BAP1, but not inactivating mutant BAP1, prominently

BAP1 suppresses HCC invasion by deubiquitinating PTEN

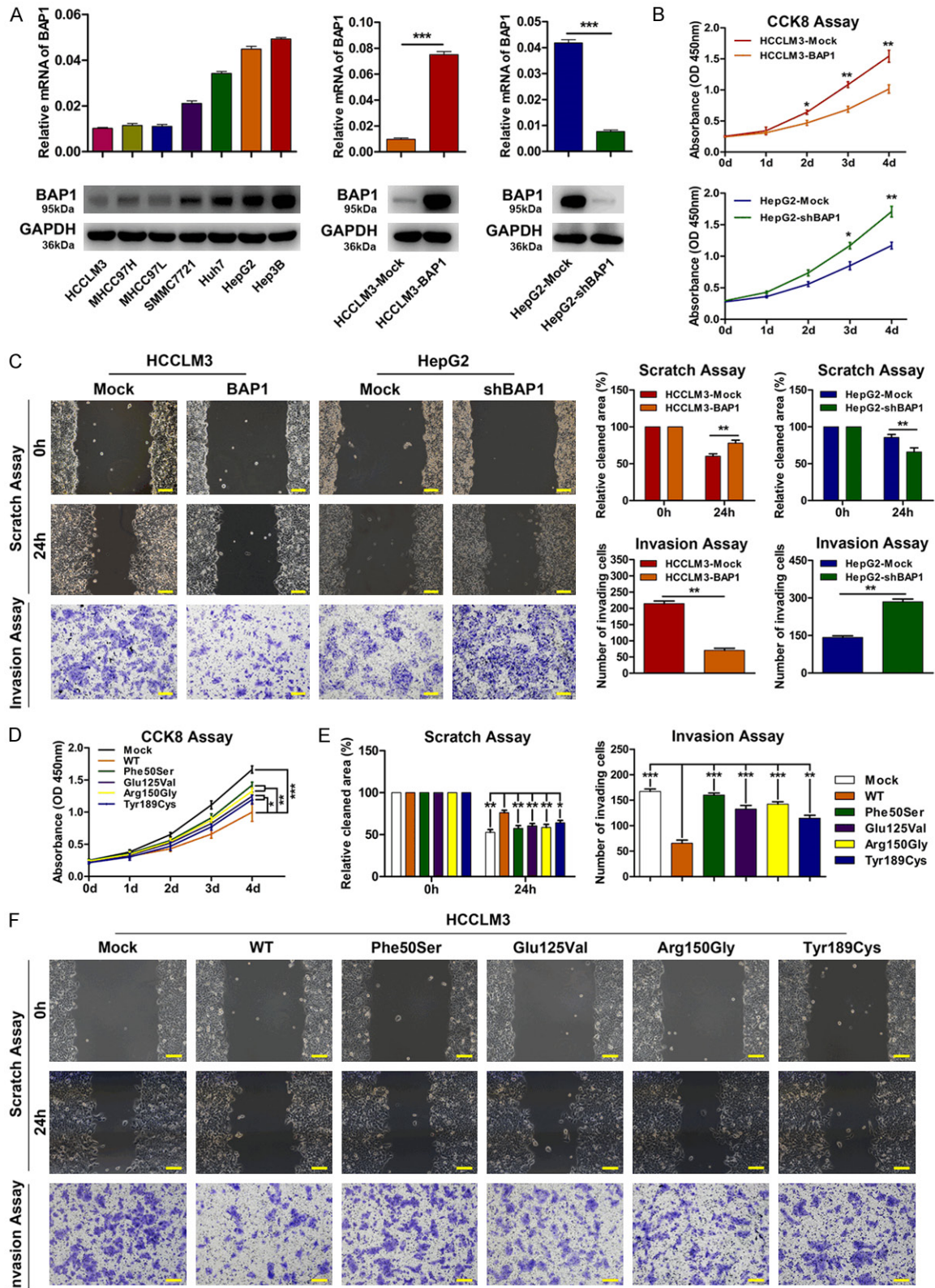


Figure 4. BAP1 deficiency enhanced HCC progression and metastasis *in vitro*. A. The expression level of BAP1 mRNA and protein in indicated HCC cell lines. B. Effects of overexpressing and downregulating BAP1 on HCC cell proliferation by using CCK8 assay. C. Effects of overexpressing and downregulating BAP1 on HCC cell migration and invasion by using scratch assay and Matrigel invasion assay, respectively. D. Effects of overexpression of WT BAP1 and mu-

BAP1 suppresses HCC invasion by deubiquitinating PTEN

tant BAP1 on cell proliferation using CCK8 assay. E and F. Effects of overexpression of WT BAP1 and mutant BAP1 on cell migration and invasion using scratch assay and Matrigel invasion assay, respectively. Scale bars = 200 μm . Bar graphs described quantification of three independent results. * $P < 0.05$, ** $P < 0.01$, *** $P < 0.001$.

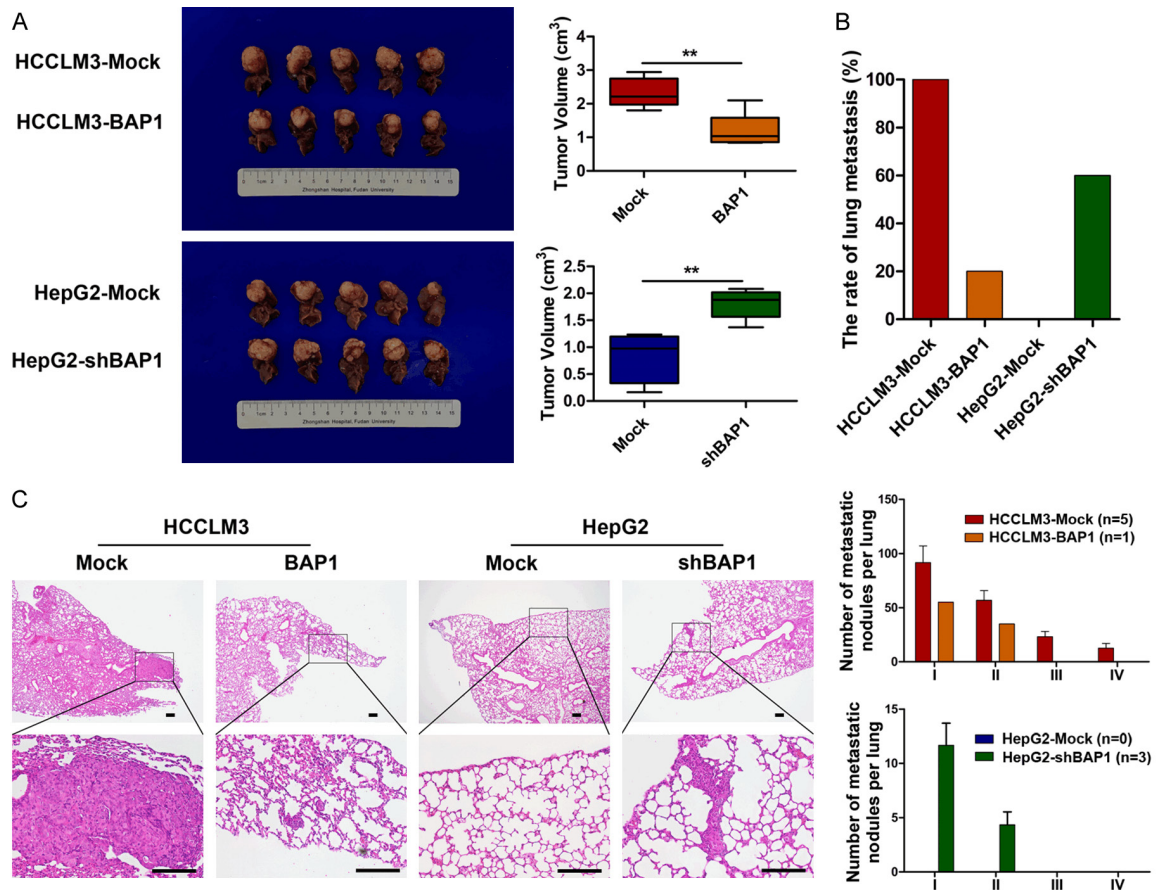


Figure 5. BAP1 deficiency enhanced HCC progression and metastasis *in vivo*. A. Representative xenograft tumors originated from indicated HCC cell lines (Left panel). Tumor volume of the tumors was gauged at 6 weeks (Right panel). B. Incidence of lung metastasis among the different animal groups. C. Representative IHC images of hematoxylin-eosin staining of lung metastatic nodules in different animal groups (Left panel). The grades of lung metastatic nodules in each animal group were shown (Right panel). Scale bars = 200 μm . Data depicted the mean \pm SD (n = 5) and were represented quantification of three independent results. ** $P < 0.01$.

increased the stability of endogenous PTEN protein (Figure 7D).

Conversely, knockdown of endogenous BAP1 markedly decreased the stability of endogenous PTEN protein in HepG2 cells (Figure 7D).

Moreover, to validate the correlation of BAP1 and PTEN expression in HCC, we further performed IHC staining of BAP1 and PTEN in TMAs containing a cohort of 396 HCC patients. Likewise, IHC results demonstrated that the expression of BAP1 and PTEN were positively correlated with each other in HCC (Figure 7E; Table S6). To assess the combined effects of BAP1 and PTEN on the postoperative survival

of HCC, the 396 patients with HCC were categorized into three groups as follows based on the BAP1 and PTEN expression: HCC patients with both high BAP1 and PTEN expression were classified as group I; HCC patients with both low BAP1 and PTEN were classified as group III; the other HCC patients were classified as group II. Strikingly, HCC patients in group I had better OS and RFS than HCC patients in group II or group III (Figure 7F).

BAP1 deficiency led to activation of AKT signaling and induction of EMT

AKT signaling is an important downstream target of PTEN, and AKT/GSK-3 β /Snail signaling

BAP1 suppresses HCC invasion by deubiquitinating PTEN

PTEN, or E3 ligase WWP2, and the indicated cell lysates were analyzed by western blot. C. HCCLM3 cells were transfected with PTEN, Ub, WT BAP1, or mutant BAP1. HepG2 cells were transfected with shBAP1 and Ub. All the cells were treated by MG132 (10 mM, 6 h) before collection, immunoprecipitated by PTEN antibody and immunoblotted with Ub and PTEN antibodies. D. HCCLM3 cells were transfected with WT BAP1 or mutant BAP1, treated by cycloheximide (CHX) for indicated times before collection, and then immunoblotted with BAP1, PTEN and GAPDH antibodies (Upper panel). HepG2 cells were transfected with shBAP1, treated by cycloheximide (CHX) before collection for indicated times, and then immunoblotted with BAP1, PTEN and GAPDH antibodies (Lower panel). The protein level of PTEN was expressed relative to GAPDH in the densitometry analysis. E. Immunostaining images of BAP1 and PTEN in representative HCC patients using Serial HCC sections. Patient 1 had high expression of BAP1 and PTEN, whereas patient 2 had low expression of BAP1 and PTEN. Scale bars = 50 μ m. F. Prognostic values of BAP1 and PTEN in HCC by Kaplan-Meier survival analysis. I, BAP1^{high} and PTEN^{high}; III, BAP1^{low} and PTEN^{low}; and II, others. Bar graphs described quantification of three independent results. * $P < 0.05$, ** $P < 0.01$, *** $P < 0.001$.

activated AKT/GSK-3 β /Snail signaling and induced EMT in HCC.

PTEN protein level is vital for BAP1-regulated EMT and cell invasion

To elucidate the role of PTEN in EMT and cell invasion regulated by BAP1 in HCC, we transfected shPTEN into HCCLM3-BAP1 cells to inhibit of PTEN expression. Interestingly, shPTEN transfection in HCCLM3-BAP1 cells induced evident cell morphology change from epithelial to fibroblastic phenotype, reversing the morphology change caused by BAP1 overexpression (Figure S4A). Consistent changes in key molecular markers of EMT and activating AKT/GSK-3 β /Snail signaling were also observed in these cells, and the proliferation, migratory and invasive capacities of these cells were significantly enhanced (Figures 8C, S5A). However, after we treated these cells using AKT inhibitor MK2206, the effects of shPTEN in HCCLM3-BAP1 cells were abolished, thus indicating that activating AKT/GSK-3 β /Snail signaling was necessary for HCC cell invasion and EMT (Figures 8C, S4A, S5A). To further validate these findings, we also transfected PTEN into HepG2-shBAP1 cells. As expected, PTEN overexpression in HepG2-shBAP1 cells obviously induced cell morphology change from fibroblastic to epithelial phenotype, reversing the morphology change caused by BAP1 downregulation (Figure S4B). Simultaneous changes in key molecular markers of EMT were consistently observed in these cells, which also showed inactivating AKT/GSK-3 β /Snail signaling (Figure 8D). Moreover, PTEN overexpression markedly suppressed cell viability, proliferation, migration and invasion of HepG2-shBAP1 cells (Figures 8D, S5B). These findings supported the crucial role of PTEN in BAP1-regulated EMT and cell invasion.

Discussion

In our study, we systematically investigated the biological significance as well as the underlying mechanisms of BAP1 and its mutants in HCC progression and metastasis. The results demonstrated that BAP1 served as a tumor suppressor in HCC, which was evidently downregulated and somatically mutated. Moreover, we also revealed that BAP1 complexed with, deubiquitinated, and stabilized PTEN to inhibit EMT and cell invasion in HCC.

Initiation and progression of HCC is considered a complex biological process partially driven by genetic alterations that activate oncogenes or inactivate tumor suppressors [17]. In our previous study, we found that BAP1 harbored recurrent somatic mutations in HCC and was defined as a potential driver gene of HCC [18]. Here, our mutation prevalence screen by Sanger sequencing showed that BAP1 was mutated in 5.71% of HCC patients, especially in those with a higher level of AFP, larger tumor bulk, greater tumor number, poorly differentiated tumor, presence of vascular invasion or tumor recurrence. The mutation frequency of BAP1 in HCC identified in our study agrees with the previous finding that identified by whole-exome sequencing [17]. Meanwhile, our study showed that BAP1 mutations were mainly missense mutations and 62.5% of which were located in the UCH domain, which were also consistent with the typical BAP1 mutation pattern in cancers [29]. Structural and functional analysis indicated that the four missense mutations located in the highly conserved UCH domain region probably harbor implied functional significance, which may inactivate BAP1 by impacting its deubiquitinase activity, structure stability, or substrate binding ability. Our subsequent experimental results confirmed the inactivating

BAP1 suppresses HCC invasion by deubiquitinating PTEN

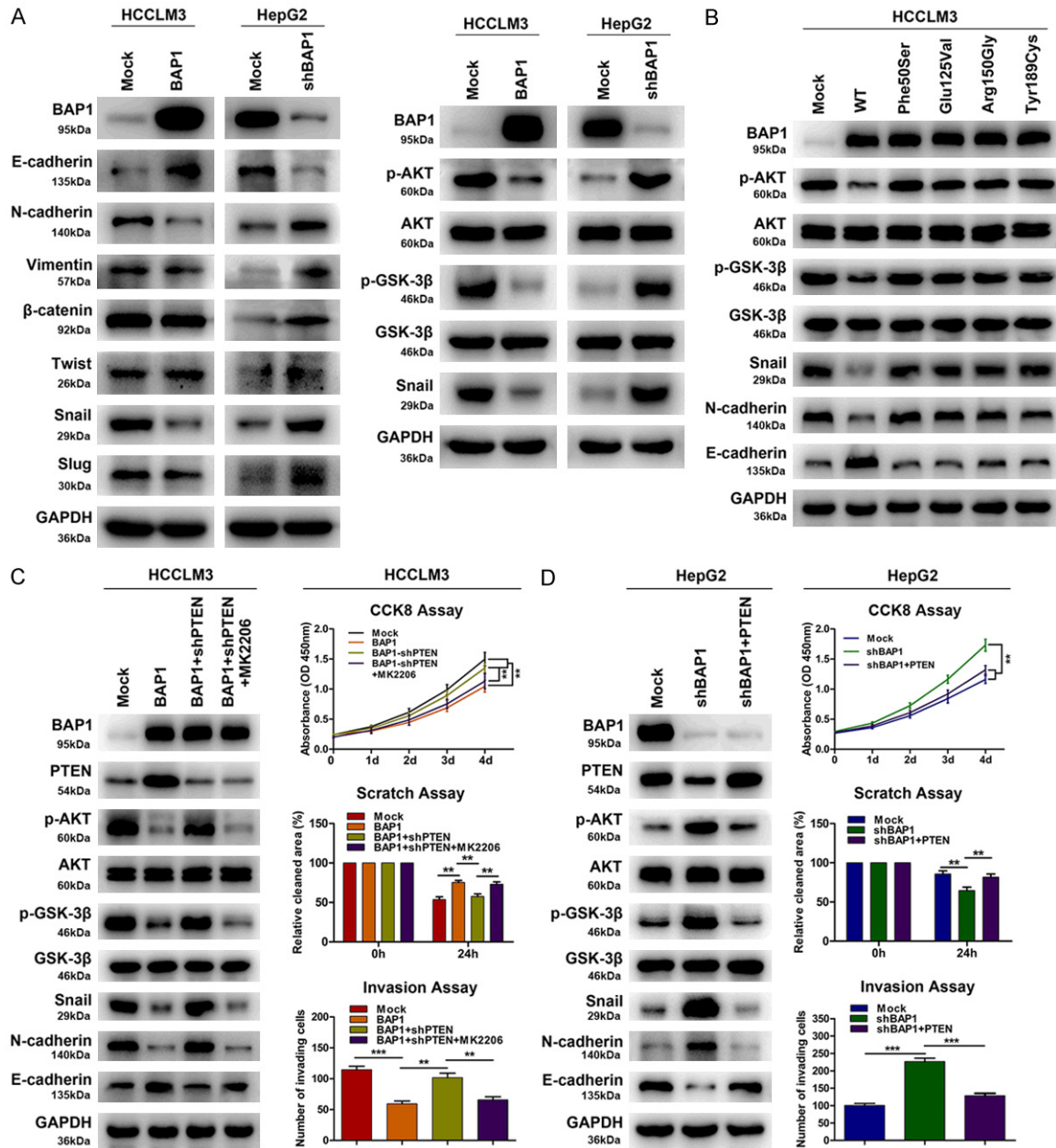


Figure 8. BAP1 deficiency induced hyperactivity of AKT signaling through PTEN, which is necessary for EMT and invasive capacity of HCC cells. A. Protein levels of the AKT/GSK-3 β /Snail signaling and the EMT markers were compared in indicated HCC cells. B. Protein levels of the AKT/GSK-3 β /Snail signaling and the key EMT markers were compared in indicated cells. C. HCCLM3-BAP1 cells were transfected with shPTEN, or treated with AKT inhibitor (MK2206) after the transfection of shPTEN. Protein levels of the AKT/GSK-3 β /Snail signaling and the key EMT markers were compared in indicated cells (Left panel). The proliferation, migratory, and invasive capacities of indicated HCC cells were examined by functional assays *in vitro* (Right panel). D. HepG2-shBAP1 cells were transfected with PTEN. Protein levels of the AKT/GSK-3 β /Snail signaling and the key EMT markers were compared in indicated cells (Left panel). The proliferation, migratory, and invasive capacities of indicated HCC cells were examined by functional assays *in vitro* (Right panel). Bar graphs described quantification of three independent results. ** $P < 0.01$, *** $P < 0.001$.

effects of somatic mutations on protein BAP1 in HCC. However, whether other mechanisms, such as posttranscriptional or epigenetic modification, inactivate protein BAP1 in HCC requires further exploration.

Credible data identified that BAP1 was obviously reduced in HCC, and its downregulation positively correlated to aggressive tumor phenotypes, such as greater tumor nodules, larger tumor bulk, appearance of vascular invasion,

BAP1 suppresses HCC invasion by deubiquitinating PTEN

and higher Chinese HCC stage, all of which are hallmarks of recurrence and poor prognosis of HCC [30]. Indeed, survival analysis confirmed that BAP1 was an independent predictor for postoperative survival, and its downregulation was associated with poor prognosis for HCC patients. Those data was in accordance with studies of other cancer types, in which tumor suppressor role of BAP1 was reported [5, 8, 9]. Furthermore, our functional assays revealed that WT BAP1 but not mutant BAP1 significantly inhibited HCC cell proliferation, invasion, EMT *in vitro*, and tumor progression and metastasis *in vivo*. Collectively, these results convinced us that BAP1 serves as a tumor suppressor of HCC and a potential treatment target for HCC.

The biological function of BAP1 in cancer always depends on its substrate proteins, and several lines of evidence in our study support BAP1 as a PTEN DUB. First, BAP1 did form a complex with PTEN. Second, BAP1 decreased PTEN polyubiquitination, and stabilized PTEN against degradation in a DUB activity-dependent manner. Third, BAP1 was downregulated and positively correlated to PTEN in human HCC; HCC patients with both high BAP1 and high PTEN expression showed the best prognosis. Finally, PTEN acts as a vital tumor suppressor in various malignancies, which is also validated in HCC [23, 31]. BAP1 inhibited cell proliferation, invasion, and EMT partially via PTEN, because overexpressing PTEN in HCC cell partially reversed the BAP1-knockdown-induced cell proliferation, invasion, and EMT, while downregulating PTEN in HCC cell partially blocked the inhibitory effects. Notably, the four missense mutations of BAP1, located in the highly conserved UCH domain region, abolished the effect that deubiquitinated and stabilized PTEN, which may attribute to that these mutations of BAP1 impacted its deubiquitinase activity or its binding with PTEN. Furthermore, as PTEN harbored loss of one allele in a large fraction of human cancers including HCC [23], we speculate that BAP1 deficiency may also drive HCC progression and metastasis with heterozygous inactivation of PTEN, and we will explore this issue in our future research projects.

Furthermore, we demonstrated that BAP1 deficiency could induce HCC cell EMT through typical EMT patterns. Overexpressing PTEN sup-

pressed the the typical EMT change in BAP1 deficient HCC cells, while knockdown of PTEN reinduced EMT in HCC cells overexpressing WT BAP1. Additionally, BAP1 has been reported to regulate various important cell signaling pathways, such as IP3R3 mediated Ca^{2+} signaling, ER stress gene-regulatory network, and the DNA damage response, etc. [5, 32-34]. Here, we showed that BAP1 negatively regulated AKT/GSK-3 β /Snail signaling by complexing with PTEN, and that BAP1 deficiency or PTEN downregulation induced activating AKT/GSK-3 β /Snail signaling was necessary for HCC cell invasion and EMT. Hence, these observations suggested that activating EMT signaling events in HCC progression caused by BAP1 deficiency are vital for HCC cell survival.

In conclusion, this study identified that BAP1 served as a tumor suppressor of HCC, which was somatically mutated and markedly down-regulated. BAP1 modulated tumor invasion and EMT by complexing with PTEN and stabilizing PTEN via deubiquitination, whereas these tumor-inhibitory effects of BAP1 were abolished by inactivating mutations. Importantly, deficiencies of BAP1 were significantly associated with aggressive tumor phenotypes, and poor postoperative prognostic outcomes. The biological features of BAP1 in HCC advocate the further investigation as a candidate treatment target for HCC.

Acknowledgements

This study was supported by the National Key R&D Program of China (2019YFC1315800, 2019YFC1315802), the State Key Program of National Natural Science of China (81830102, 81530077), the National Natural Science Foundation of China (81772578, 81902961, 81672839, 81772551, 81802991, and 816-02543), and the Sailing Program of Shanghai Science and Technology Commission (19YF14-07400 and 18YF1403600), the Strategic Priority Research Program of the Chinese Academy of Sciences (XDA12020105 and XDA12020103).

Disclosure of conflict of interest

None.

Address correspondence to: Xinrong Yang and Jian Zhou, Department of Liver Surgery and

BAP1 suppresses HCC invasion by deubiquitinating PTEN

Transplantation, Liver Cancer Institute, Zhongshan Hospital, Fudan University, 136 Yi Xue Yuan Road, Shanghai 200032, China. Tel: +86-21-64037181; Fax: +86-21-64037181; E-mail: yxr_2@163.com (XRY); zhou.jian@zs-hospital.sh.cn (JZ)

References

- [1] Forner A, Reig M and Bruix J. Hepatocellular carcinoma. *Lancet* 2018; 391: 1301-1314.
- [2] Zhou J, Sun HC, Wang Z, Cong WM, Wang JH, Zeng MS, Yang JM, Bie P, Liu LX, Wen TF, Han GH, Wang MQ, Liu RB, Lu LG, Ren ZG, Chen MS, Zeng ZC, Liang P, Liang CH, Chen M, Yan FH, Wang WP, Ji Y, Cheng WW, Dai CL, Jia WD, Li YM, Li YX, Liang J, Liu TS, Lv GY, Mao YL, Ren WX, Shi HC, Wang WT, Wang XY, Xing BC, Xu JM, Yang JY, Yang YF, Ye SL, Yin ZY, Zhang BH, Zhang SJ, Zhou WP, Zhu JY, Liu R, Shi YH, Xiao YS, Dai Z, Teng GJ, Cai JQ, Wang WL, Dong JH, Li Q, Shen F, Qin SK and Fan J. Guidelines for diagnosis and treatment of primary liver cancer in China (2017 Edition). *Liver Cancer* 2018; 7: 235-260.
- [3] European Association For The Study Of The Liver; European Organisation For Research And Treatment Of Cancer. EASL-EORTC clinical practice guidelines: management of hepatocellular carcinoma. *J Hepatol* 2012; 56: 908-943.
- [4] Llovet JM, Zucman-Rossi J, Pikarsky E, Sangro B, Schwartz M, Sherman M and Gores G. Hepatocellular carcinoma. *Nat Rev Dis Primers* 2016; 2: 16018.
- [5] Carbone M, Yang H, Pass HI, Krausz T, Testa JR and Gaudino G. BAP1 and cancer. *Nat Rev Cancer* 2013; 13: 153-159.
- [6] Luchini C, Veronese N, Yachida S, Cheng L, Nottegar A, Stubbs B, Solmi M, Capelli P, Pea A, Barbareschi M, Fassan M, Wood LD and Scarpa A. Different prognostic roles of tumor suppressor gene BAP1 in cancer: a systematic review with meta-analysis. *Genes Chromosomes Cancer* 2016; 55: 741-749.
- [7] Leblay N, Lepretre F, Le Stang N, Gautier-Stein A, Villeneuve L, Isaac S, Maillat D, Galateau-Salle F, Villenet C, Sebda S, Goracci A, Byrnes G, McKay JD, Figeac M, Glehen O, Gilly FN, Foll M, Fernandez-Cuesta L and Brevet M. BAP1 is altered by copy number loss, mutation, and/or loss of protein expression in more than 70% of malignant peritoneal mesotheliomas. *J Thorac Oncol* 2017; 12: 724-733.
- [8] Minardi D, Lucarini G, Milanese G, Di Primio R, Montironi R and Muzzonigro G. Loss of nuclear BAP1 protein expression is a marker of poor prognosis in patients with clear cell renal cell carcinoma. *Urol Oncol* 2016; 34: 338.e311-338.
- [9] Kalirai H, Dodson A, Faqir S, Damato BE and Coupland SE. Lack of BAP1 protein expression in uveal melanoma is associated with increased metastatic risk and has utility in routine prognostic testing. *Br J Cancer* 2014; 111: 1373-1380.
- [10] Boffetta P, Righi L, Ciocan C, Pelucchi C, La Vecchia C, Romano C, Papotti M and Pira E. Validation of the diagnosis of mesothelioma and BAP1 protein expression in a cohort of asbestos textile workers from Northern Italy. *Ann Oncol* 2018; 29: 484-489.
- [11] Rai K, Pilarski R, Boru G, Rehman M, Saqr AH, Massengill JB, Singh A, Marino MJ, Davidorf FH, Cebulla CM and H Abdel-Rahman M. Germline BAP1 alterations in familial uveal melanoma. *Genes Chromosomes Cancer* 2017; 56: 168-174.
- [12] Cabaret O, Perron E, Bressac-de Paillerets B, Soufir N and de la Fouchardiere A. Occurrence of BAP1 germline mutations in cutaneous melanocytic tumors with loss of BAP1-expression: a pilot study. *Genes Chromosomes Cancer* 2017; 56: 691-694.
- [13] de la Fouchardière A, Cabaret O, Savin L, Combemale P, Schvartz H, Penet C, Bonadona V, Soufir N and Bressac-de Paillerets B. Germline BAP1 mutations predispose also to multiple basal cell carcinomas. *Clin Genet* 2015; 88: 273-277.
- [14] Vignot S, Frampton GM, Soria JC, Yelensky R, Commo F, Brambilla C, Palmer G, Moro-Sibilot D, Ross JS, Cronin MT, Andre F, Stephens PJ, Lazar V, Miller VA and Brambilla E. Next-generation sequencing reveals high concordance of recurrent somatic alterations between primary tumor and metastases from patients with non-small-cell lung cancer. *J Clin Oncol* 2013; 31: 2167-2172.
- [15] Jiao Y, Pawlik TM, Anders RA, Selaru FM, Strepel MM, Lucas DJ, Niknafs N, Guthrie VB, Maitra A, Argani P, Offerhaus GJA, Roa JC, Roberts LR, Gores GJ, Popescu I, Alexandrescu ST, Dima S, Fassan M, Simbolo M, Mafficini A, Capelli P, Lawlor RT, Ruzzenente A, Guglielmi A, Tortora G, de Braud F, Scarpa A, Jarnagin W, Klimstra D, Karchin R, Velculescu VE, Hruban RH, Vogelstein B, Kinzler KW, Papadopoulos N and Wood LD. Exome sequencing identifies frequent inactivating mutations in BAP1, ARID1A and PBRM1 in intrahepatic cholangiocarcinomas. *Nat Genet* 2013; 45: 1470-1473.
- [16] Pena-Llopis S, Vega-Rubin-de-Celis S, Liao A, Leng N, Pavia-Jimenez A, Wang S, Yamasaki T, Zhrebker L, Sivanand S, Spence P, Kinch L, Hambuch T, Jain S, Lotan Y, Margulis V, Sgallowsky AI, Summerour PB, Kabbani W, Wong SW, Grishin N, Laurent M, Xie XJ, Haudenschild CD, Ross MT, Bentley DR, Kapur P and Bruga-

BAP1 suppresses HCC invasion by deubiquitinating PTEN

- rolas J. BAP1 loss defines a new class of renal cell carcinoma. *Nat Genet* 2012; 44: 751-759.
- [17] Cancer Genome Atlas Research Network. Electronic address: wheeler@bcm.edu; Cancer Genome Atlas Research Network. Comprehensive and integrative genomic characterization of hepatocellular carcinoma. *Cell* 2017; 169: 1327-1341, e23.
- [18] Huang A, Zhao X, Yang XR, Li FQ, Zhou XL, Wu K, Zhang X, Sun QM, Cao Y, Zhu HM, Wang XD, Yang HM, Wang J, Tang ZY, Hou Y, Fan J and Zhou J. Circumventing intratumoral heterogeneity to identify potential therapeutic targets in hepatocellular carcinoma. *J Hepatol* 2017; 67: 293-301.
- [19] Wittekind C. Pitfalls in the classification of liver tumors. *Pathologe* 2006; 27: 289-293.
- [20] Yang XR, Xu Y, Yu B, Zhou J, Qiu SJ, Shi GM, Zhang BH, Wu WZ, Shi YH, Wu B, Yang GH, Ji Y and Fan J. High expression levels of putative hepatic stem/progenitor cell biomarkers related to tumour angiogenesis and poor prognosis of hepatocellular carcinoma. *Gut* 2010; 59: 953-962.
- [21] Adzhubei IA, Schmidt S, Peshkin L, Ramensky VE, Gerasimova A, Bork P, Kondrashov AS and Sunyaev SR. A method and server for predicting damaging missense mutations. *Nat Methods* 2010; 7: 248-249.
- [22] Fraile JM, Quesada V, Rodriguez D, Freije JM and Lopez-Otin C. Deubiquitinases in cancer: new functions and therapeutic options. *Oncogene* 2012; 31: 2373-2388.
- [23] Song MS, Salmena L and Pandolfi PP. The functions and regulation of the PTEN tumour suppressor. *Nat Rev Mol Cell Biol* 2012; 13: 283-296.
- [24] Maddika S, Kavela S, Rani N, Palicharla VR, Pokorny JL, Sarkaria JN and Chen J. WWP2 is an E3 ubiquitin ligase for PTEN. *Nat Cell Biol* 2011; 13: 728-733.
- [25] Ahmed SF, Deb S, Paul I, Chatterjee A, Mandal T, Chatterjee U and Ghosh MK. The chaperone-assisted E3 ligase C terminus of Hsc70-interacting protein (CHIP) targets PTEN for proteasomal degradation. *J Biol Chem* 2012; 287: 15996-16006.
- [26] Lee JT, Shan J, Zhong J, Li M, Zhou B, Zhou A, Parsons R and Gu W. RFP-mediated ubiquitination of PTEN modulates its effect on AKT activation. *Cell Res* 2013; 23: 552-564.
- [27] Zhang B, Yin C, Li H, Shi L, Liu N, Sun Y, Lu S, Liu Y, Sun L, Li X, Chen W and Qi Y. Nir1 promotes invasion of breast cancer cells by binding to chemokine (C-C motif) ligand 18 through the PI3K/Akt/GSK3beta/Snail signalling pathway. *Eur J Cancer* 2013; 49: 3900-3913.
- [28] Jin J, Zhang Z, Zhang S, Chen X, Chen Z, Hu P, Wang J and Xie C. Fatty acid binding protein 4 promotes epithelial-mesenchymal transition in cervical squamous cell carcinoma through AKT/GSK3beta/Snail signaling pathway. *Mol Cell Endocrinol* 2018; 461: 155-164.
- [29] Murali R, Wiesner T and Scolyer RA. Tumours associated with BAP1 mutations. *Pathology* 2013; 45: 116-126.
- [30] Marrero JA, Kulik LM, Sirlin C, Zhu AX, Finn RS, Abecassis MM, Roberts LR and Heimbach JK. Diagnosis, staging and management of hepatocellular carcinoma: 2018 practice guidance by the American association for the study of liver diseases. *Hepatology* 2018; 68: 723-750.
- [31] Khalid A, Hussain T, Manzoor S, Saalim M and Khaliq S. PTEN: a potential prognostic marker in virus-induced hepatocellular carcinoma. *Tumour Biol* 2017; 39: 1010428317705754.
- [32] Dai F, Lee H, Zhang Y, Zhuang L, Yao H, Xi Y, Xiao ZD, You MJ, Li W, Su X and Gan B. BAP1 inhibits the ER stress gene regulatory network and modulates metabolic stress response. *Proc Natl Acad Sci U S A* 2017; 114: 3192-3197.
- [33] Bononi A, Giorgi C, Patergnani S, Larson D, Verbruggen K, Tanji M, Pellegrini L, Signorato V, Olivetto F, Pastorino S, Nasu M, Napolitano A, Gaudino G, Morris P, Sakamoto G, Ferris LK, Danese A, Raimondi A, Tacchetti C, Kuchay S, Pass HI, Affar EB, Yang H, Pinton P and Carbone M. BAP1 regulates IP3R3-mediated Ca(2+) flux to mitochondria suppressing cell transformation. *Nature* 2017; 546: 549-553.
- [34] Yu H, Pak H, Hammond-Martel I, Ghram M, Rodrigue A, Daou S, Barbour H, Corbeil L, Hebert J, Drobetsky E, Masson JY, Di Noia JM and Affar el B. Tumor suppressor and deubiquitinase BAP1 promotes DNA double-strand break repair. *Proc Natl Acad Sci U S A* 2014; 111: 285-290.

Supplementary Materials and Methods

Tissue microarray construction and immunohistochemistry

Tissue microarrays (TMAs) were constructed as described in our previous study [1]. Archived paraffin-embedded tissue samples from 396 HCC patients treated with curative resection in Liver Cancer Institute, Zhongshan Hospital, Fudan University (Shanghai, China) between 2000 and 2002 were selected for TMA construction. Core samples were obtained from representative regions of each tumor tissue and matched adjacent non-tumor liver tissue, which is specifically identified by hematoxylin and eosin staining. Duplicate 1 mm cores were taken from different regions of the same tissue block for each case (tumor tissue and matched non-tumor liver tissue, a total of four cores for one case). Subsequently, TMAs were constructed using an arraying machine (Beecher Instruments, USA).

Immunohistochemical staining was performed using the avidin-biotin-peroxidase complex method as described previously [1]. Briefly, after rehydration and microwave antigen retrieval, primary antibodies were applied to slides, incubated at 4°C overnight, and followed with secondary antibody incubation (Gene Tech, China) at 37°C for 30 min. Then, staining was carried out with DAB and counter-staining with Mayer's hematoxylin. Negative control slides with the primary antibodies omitted were included in all assays. Immunostaining intensities of these markers were semiquantitatively scored as follows: 0, negative; 1, weak; 2, moderate; 3, strong [2]. The score of immunostaining intensity was assessed by two observers independently, and comparisons were made between tumor/normal pairs. In the survival analyses, scores 0 and 1 were defined as low expression, whereas scores 2 and 3 were defined as high expression.

Screening of mutations using sanger sequencing

To investigate the prevalence of BAP1 mutation in HCC, all the 17 coding exons of BAP1 were screened using Sanger sequencing in the 105 HCC samples and matched adjacent non-tumor liver tissues. The PCR primers used for Sanger sequencing were listed in [Table S4](#). Sanger sequencing primers were designed using Primer3 software (<http://frodo.wi.mit.edu/>). All mutations identified in tumors were confirmed by independent PCR and Sanger sequencing in the matched adjacent non-tumor liver tissues to determine their somatic nature.

Protein structural analysis and sequence alignment analysis

To decipher the potential structural and functional impact of the mutations identified by Sanger sequencing in HCC, the three-dimensional structure models of BAP1 were generated by the softwares such as FR-t5-M and I-TASSER, based on the template protein (PDB ID: 3IHR) which is a deubiquitylating enzyme UCH37 [3-5]. The wild and mutate type of BAP1 were optimized by side-chain packing program CIS-RR [6]. Pymol software (www.pymol.org/) was used to draw the structure models. Furthermore, ClustalX was used to align the sequences of homologous BAP1 proteins among different vertebrate species [7].

Cell lines and transfection

Human HCC cell lines SMMC7721, Huh7, HepG2, and Hep3B, were purchased from Chinese Academy of Sciences Shanghai Branch Cell Bank, Shanghai, China. Human HCC cell lines MHCC97L, MHCC97H and HCCLM3, were established in our institute. All cell lines were cultured in Dulbecco's modified Eagle's medium (Invitrogen, USA) supplemented with 10% fetal bovine serum (Gibco, USA) and penicillin/streptomycin.

Lentiviral vector encoding wild-type (WT) BAP1 for overexpression of BAP1 was transfected into HCCLM3 cells and designated as HCCLM3-BAP1 cells. HCCLM3-Mock cells, which were transfected with lentiviral vector alone, were used as control. WT BAP1 complementary DNA was amplified by polymerase chain reaction (PCR) from complementary DNA of the HCCLM3 cell line. Constructs encoding the Phe50Ser, Glu125Val, Arg150Gly, and Tyr189Cys BAP1 variants were generated as previously described

BAP1 suppresses HCC invasion by deubiquitinating PTEN

[8], and then cloned into pcDNA3.1 vector and transfected into HCCLM3 cells using Lipofectamine 2000 (Invitrogen, USA) reagent following the manufacturer's instructions. Moreover, lentiviral vectors encoding PTEN, WWP2, and Ub were also constructed and transfected into indicated HCC cells. Lentiviral vector encoding short hairpin (sh) BAP1 for downregulation of BAP1 was transfected into HepG2 cells and designated as HepG2-shBAP1. HepG2-Mock cells, which were transfected with lentiviral vector alone, were used as control. Lentiviral vectors encoding shPTEN was transfected into HCCLM3 cells for downregulation of PTEN. Stably transfected clones were validated by real-time quantitative reverse transcription PCR (qRT-PCR), western blot, or immunofluorescence assays.

RNA isolation and quantitative reverse transcription PCR (qRT-PCR)

Total RNA was extracted using Trizol reagent (Invitrogen, USA) and reverse transcribed to cDNA using PrimeScript RT reagent kit (Takara, Japan) following the manufacturer's instructions. SYBR Premix Ex Taq™ (Takara, Japan) was used for real time RT-PCR, and gene amplification and detection were performed using the ABI PRISM 7900 Sequence Detection System (Applied Biosystems, USA). Gene transcription level was normalized to Glyceraldehyde 3-phosphate dehydrogenase (GAPDH) expression. Gene specific primers were designed as follows: BAP1 Forward 5'-GACCCAGGCCTCTTACC-3'; BAP1 Reverse 5'-AGTCCTTCATGCGACTCAGG-3'; GAPDH Forward 5'-AGCCACATCGCTCAGACAC-3'; GAPDH Reverse 5'-GAATTTGCCATGGGTGGA-3'.

Western blot and immunofluorescence assay

Protein extracts from tissues or cells were separated on 10% sodium dodecyl sulfate-polyacrylamide gel electrophoresis (SDS-PAGE), and subsequently transferred onto polyvinylidene difluoride (PVDF) membranes. Then, the membranes were blocked, and further incubated with corresponding primary antibodies followed by respective secondary antibodies. Finally, immunoreactive bands were detected by enhanced chemiluminescence assays. GAPDH was used as the loading control. Cells were fixed with 4% paraformaldehyde for 30 min, washed with PBS, permeabilized with 0.1% Triton X-100 for 15 min, and blocked with PBS containing 5% bovine serum albumin (BSA) for 1 h, and then incubated with corresponding primary antibodies followed by respective secondary antibodies. Then, the slices were stained with diamidino phenylindole (DAPI) and observed using fluorescence microscopy (Leica Microsystems Imaging Solutions, UK). For each channel, images were acquired with the same settings.

Immunoprecipitation assays

Cells were collected and lysed in IP lysis buffer with protease inhibitors (Cell Signaling Technology, USA). Then, cell extracts were incubated with indicated primary antibody followed by protein-A/G beads (Santa Cruz Biotechnology, USA). The precipitates were washed with IP lysis buffer, and eluted by boiling in 2×SDS sample buffer followed by SDS-PAGE and western blot analysis.

Deubiquitylation assays

Indicated cells were treated with 10 μM MG132 (Selleck, USA) for 6 h to inhibit proteasome activity. Then, cells were lysed and immunoprecipitated with indicated primary antibody followed by protein-A/G beads (Santa Cruz Biotechnology, USA). Finally, the bound proteins proceed to western blot and detect the ubiquitin.

Cell proliferation assay, migration assay, and matrigel invasion assay

Cells (2000 cells/well) were aliquoted into a 96-well plate and incubated for indicated time. 10 μl Cell Counting Kit 8 (CCK8) solution (Dojindo, Japan) was added at the indicated time points, and then incubated for further 2 hours. Absorbance at 450 nm was measured to determine the cell viability and growth.

Scratch assay were used to detect cell migration. Cells were cultured to form a tight cell monolayer in a 6-well plate. Then, the cell monolayer was scratched with a sterile 200 μl pipette tip to create a "wound-

BAP1 suppresses HCC invasion by deubiquitinating PTEN

ing” line. The cleaned area at indicated time point was measured and photographed using a microscope (Leica Microsystems Imaging Solutions, UK). The cleaned area at each time point was normalized to those at time zero.

Matrigel invasion assays were conducted using 8 μ m pore size 24-well transwells (Corning, USA) pre-coated with Matrigel (BD Biosciences, USA). Cells (8×10^4 cells/transwell) were suspended in 200 μ l Dulbecco’s modified Eagle medium (DMEM) with 1% fetal bovine serum (FBS) and added to the upper chamber; 600 μ l DMEM with 10% FBS was added in the lower chamber. Following an incubation period, the cells on the lower surface of the membrane were fixed, stained, counted and photographed using a microscope (Leica Microsystems Imaging Solutions, UK).

***In vivo* assays**

Male BALB/C nude mice (4-6 weeks old) were purchased from the Shanghai Institute of Material Medicine of the Chinese Academy of Science and housed in specific pathogen-free conditions. Animal care and experimental protocols were performed following guidelines established by the Shanghai Medical Experimental Animal Care Commission. Ethical approval was obtained from the research ethics committee of Zhongshan Hospital. Indicated cells were trypsinized, resuspended in 200 μ l serum-free DMEM, then injected subcutaneously into the upper left flank region of nude mice. When the subcutaneous tumors reached approximately 1 cm in length (approximately 4 weeks after injection), the tumors were removed and orthotopic liver transplantation models were performed according to standard procedures described previously [9]. At the end of study, mice were sacrificed and tumor tissues were removed, measured, and photographed. The volume of tumors was calculated in cm^3 using the following formula: $V = \text{length} \times \text{width}^2/2$. Lungs were removed and embedded in paraffin; the total number of lung metastases was counted under the microscope as described previously [10].

Statistical analysis

Statistical analyses were performed using SPSS version 18.0 software. Categorical data were analyzed using the chi-square test or Fisher exact test and continuous data were analyzed using the Student’s t-test or one-way analysis of variance, when appropriate. OS and RFS curves were plotted using the Kaplan-Meier method, and differences were analyzed using the log-rank test. The Cox proportional hazards regression model was used for all the univariate and multivariate analyses. Two-tailed *P* values less than 0.05 were considered statistically significant.

References

- [1] Yang XR, Xu Y, Yu B, Zhou J, Qiu SJ, Shi GM, Zhang BH, Wu WZ, Shi YH, Wu B, Yang GH, Ji Y and Fan J. High expression levels of putative hepatic stem/progenitor cell biomarkers related to tumour angiogenesis and poor prognosis of hepatocellular carcinoma. *Gut* 2010; 59: 953-962.
- [2] Seidal T, Balaton AJ and Battifora H. Interpretation and quantification of immunostains. *Am J Surg Pathol* 2001; 25: 1204-1207.
- [3] Dai W, Song T, Wang X, Jin X, Deng L, Wu A and Jiang T. Improvement in low-homology template-based modeling by employing a model evaluation method with focus on topology. *PLoS One* 2014; 9: e89935.
- [4] Dai W, Wu A, Ma L, Li YX, Jiang T and Li YY. A novel index of protein-protein interface propensity improves interface residue recognition. *BMC Syst Biol* 2016; 10: 112.
- [5] Yang J, Yan R, Roy A, Xu D, Poisson J and Zhang Y. The I-TASSER Suite: protein structure and function prediction. *Nat Methods* 2015; 12: 7-8.
- [6] Cao Y, Song L, Miao Z, Hu Y, Tian L and Jiang T. Improved side-chain modeling by coupling clash-detection guided iterative search with rotamer relaxation. *Bioinformatics* 2011; 27: 785-790.
- [7] Larkin MA, Blackshields G, Brown NP, Chenna R, McGettigan PA, McWilliam H, Valentin F, Wallace IM, Wilm A, Lopez R, Thompson JD, Gibson TJ and Higgins DG. Clustal W and Clustal X version 2.0. *Bioinformatics* 2007; 23: 2947-2948.
- [8] Yang LX, Gao Q, Shi JY, Wang ZC, Zhang Y, Gao PT, Wang XY, Shi YH, Ke AW, Shi GM, Cai JB, Liu WR, Duan M, Zhao YJ, Ji Y, Gao DM, Zhu K, Zhou J, Qiu SJ, Cao Y, Tang QQ and Fan J. Mitogen-activated protein kinase kinase 4 deficiency in intrahepatic cholangiocarcinoma leads to invasive growth and epithelial-mesenchymal transition. *Hepatology* 2015; 62: 1804-1816.

BAP1 suppresses HCC invasion by deubiquitinating PTEN

- [9] Zhou SL, Dai Z, Zhou ZJ, Wang XY, Yang GH, Wang Z, Huang XW, Fan J and Zhou J. Overexpression of CXCL5 mediates neutrophil infiltration and indicates poor prognosis for hepatocellular carcinoma. *Hepatology* 2012; 56: 2242-2254.
- [10] Tian J, Tang ZY, Ye SL, Liu YK, Lin ZY, Chen J and Xue Q. New human hepatocellular carcinoma (HCC) cell line with highly metastatic potential (MHCC97) and its expressions of the factors associated with metastasis. *Br J Cancer* 1999; 81: 814-821.

Table S1. Sequence of primers for construction of BAP1 variants

Clone	Forward primer (5'-3')	Reverse primer (5'-3')
WT	GGCTGCAGTGCAGCTAGACGCCACCATGAATAAGGGCTGGCTGGAGCTGG	ATAGCGCTACCCGGGATCCCTGGCGCTTGGCCTTGTAGGGGCGAG
Phe50Ser	ATCTTCCTGTCCAAATGATCGAAGAGCGCCGGTCC	CGATCCATTGGACAGGAAGATAAATCCATATACAG
Glu125Val	GTTTCAGCCCTGTGAGCAAAGGATATGCGATTGGC	CCTTTGCTCACAGGGCTGAAACCCCTGGTGAAG
Arg150Gly	GCCCGAGCCAGGCCACCTCCCTGAGAAGCAGAATG	AGGGAGGTGGCTGGCTCGGGCCTGGCATGGC
Tyr189Cys	CTGAAGGTCTGCCCATTTACCATGGGCCCTGG	GTCAATGGGGCAGACCTTCAGCCCATCCAGCTC

Abbreviations: WT, wild type.

Table S2. Target sequences of shBAP1 and shPTEN

Gene	List	Target sequence (5'-3')
BAP1	sh1	ACAACACTACGATGAGTTCAT
	sh2	TGGAAGATTTCCGGTGTCAA
	sh3	TCCGTGATTGATGATGATA
PTEN	sh1	AGAGATCGTTAGCAGAAAC
	sh2	GTATAGAGCGTGCAGATAA
	sh3	AGAACTTATCAAACCCCTTT

Abbreviations: sh, short hairpin.

Table S3. Primary antibodies for WB, co-IP, IHC, and IF

Antibody	Concentration for WB	Concentration for co-IP	Concentration for IHC	Concentration for IF	Specificity	Company	RRID
BAP1	/	/	1:100	1:50	Mouse	Santa cruz	AB_626723
BAP1	1:1000	1:50	/	/	Rabbit	CST	AB_2798168
GAPDH	1:100	/	/	/	Mouse	Santa cruz	AB_10847862
IgG	/	1:50	/	/	Rabbit	CST	AB_1550038
PTEN	1:1000	1:50	/	/	Rabbit	CST	AB_390810
N-cadherin	1:1000	/	/	/	Rabbit	CST	AB_2687616
E-cadherin	1:1000	/	/	/	Rabbit	CST	AB_2291471
Vimentin	1:1000	/	/	/	Rabbit	CST	AB_10695459
β -catenin	1:1000	/	/	/	Rabbit	CST	AB_11127855
Twist	1:1000	/	/	/	Rabbit	CST	AB_2799308
Snail	1:1000	/	/	/	Rabbit	CST	AB_2255011
Slug	1:1000	/	/	/	Rabbit	CST	AB_2239535
AKT	1:1000	/	/	/	Rabbit	CST	AB_915783
p-AKT ^{Ser473}	1:1000	/	/	/	Rabbit	CST	AB_2224726
GSK-3	1:1000	/	/	/	Rabbit	CST	AB_2636978
p-GSK-3 ^{Ser9}	1:1000	/	/	/	Rabbit	CST	AB_2798546
WWP2	1:2000	/	/	/	Rabbit	Abcam	AB_10710285
Ub	1:1000	/	/	/	Mouse	CST	AB_331292

Abbreviations: CST, Cell Signaling Technology; IF, immunofluorescence; IHC, immunohistochemistry; IP, immunoprecipitation; Santa cruz, Santa Cruz Biotechnology; Ub, ubiquitin; WB, western blot.

BAP1 suppresses HCC invasion by deubiquitinating PTEN

Table S4. List of PCR primers for Sanger sequencing

Amplification NO.	Exon	Forward primer (5'-3')	Reverse primer (5'-3')	Amplification Length (bp)
1	1/2/3	GGGAGAAGACAATCAGCA	AGAGCGACCCAGGTGAGGAG	1210
		CCCCTTGACACCTGCGATGA	GAGCGCATGCCCGCATCTG	508
2	4	TGGAGCATCACAGTCAGA	AACAAGCACCTACCAAATAC	608
3	5	GAAAGGAGCTGAGAAGGG	AGGAATCGGAAGGAACAC	648
4	6/7	GCCAGCACAGTCCATCTC	CCTCCCAAAGTAGGTACAGC	877
5	8	TCCCTGAGAAGCAGAATGG	AAGACAACAAGTTGAGAACCC	622
6	9	CAGGTCTGCTGGTTCACTT	GCTCTACCCATTCACTCACA	590
7	10	GGAGCCCTACCACGACAT	GGAAGAACACTGCCCAAG	727
8	11	TTTCCCATCTCATTCTTTGC	GGCTGCCACCCACTTACA	739
9	12	GTTTCAGGGCACTCTGTTT	CACCCACATCTCCTCCAT	643
10	13	GAGCACCTGCGGAGTTTG	GCGAGTCCATGCCTATCAA	1394
11	14	TGTCACCTCCACATCTCC	ACCACCCAACCCAGAAAG	591
12	15/16	ACTTTCTGGGTTGGGTGGTG	CAGGCTTCGCTGCTTGT	676
13	17	CTGCTCTGGCAAGATTGG	AGGGCACGATGGAAGGAA	602

Table S5. Relationship of BAP1 mutation (n = 6) with clinicopathological characteristics of HCC (n = 105)

AFP		Tumor size		Tumor number	
-	+	≤5 cm	>5 cm	Single	Multiple
2.1% (1/47)	8.6% (5/58)	3.2% (2/63)	9.5% (4/42)	4.4% (4/91)	14.3% (2/14)
Tumor differentiation		Vascular invasion*		Recurrence	
I-II	III-IV	-	+	-	+
4.2% (3/72)	9.1% (3/33)	1.4% (1/70)	14.3% (5/35)	4.1% (2/49)	7.1% (4/56)

Abbreviations: AFP, alpha-fetoprotein. * $P = 0.015$, and $P > 0.05$ for all the other analysis (Fisher's exact tests).

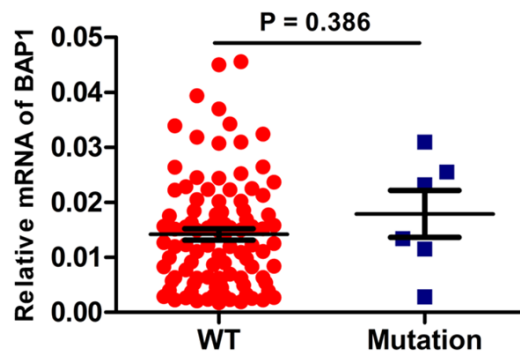


Figure S1. The relevance of mutation versus expression of BAP1 in HCC (WT: n = 99; Mutation: n = 6). All bar graphs depicted quantification of triplicate results with mean \pm SD. Abbreviations: WT, wild type.

BAP1 suppresses HCC invasion by deubiquitinating PTEN

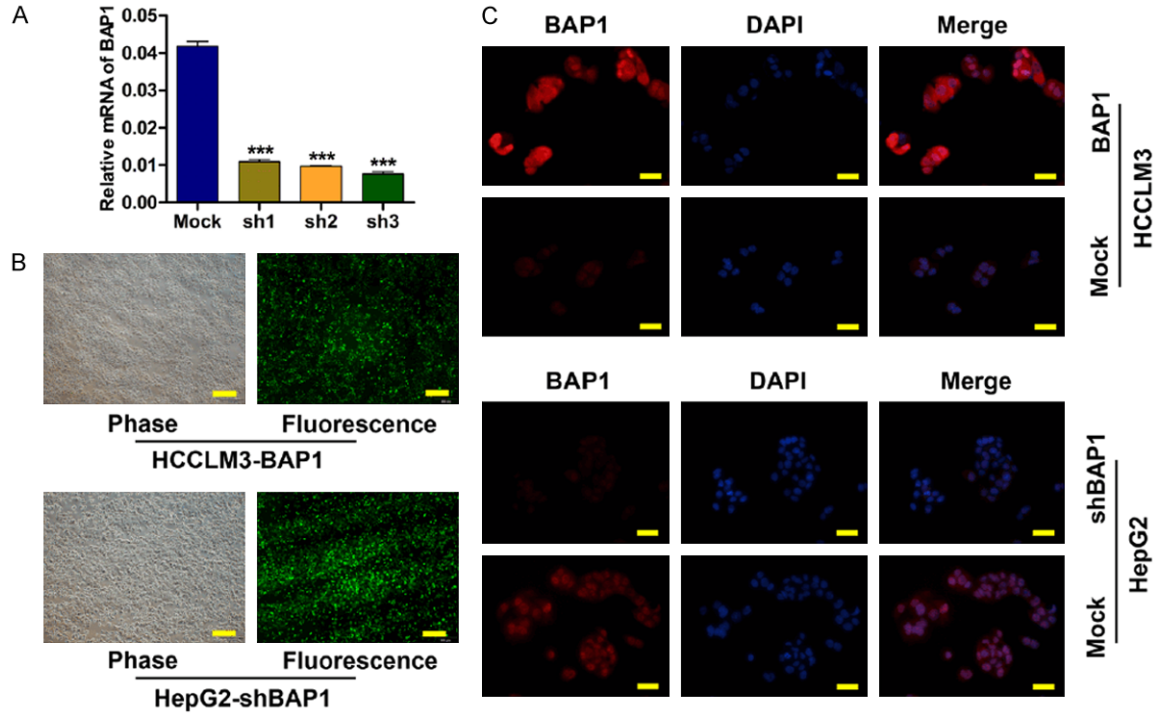


Figure S2. The transfection efficiency of lentiviral vectors. A. The mRNA expression of BAP1 in indicated HepG2 cells transfected with shBAP1 vectors or vector control. B. The transfection efficiency of HCCLM3-BAP1 and HepG2-shBAP1 were evaluated by immunofluorescent staining (EGFP in the lentiviral vector). Scale bars = 500 μ m. C. The transfection efficiency of HCCLM3-BAP1 and HepG2-shBAP1 were evaluated by immunofluorescent staining (Using specific BAP1 antibody). Scale bars = 100 μ m. A representative image in each group is illustrated. All bar graphs depicted quantification of triplicate results with mean \pm SD. *** P <0.001. Abbreviations: DAPI, 4',6-diamidino-2-phenylindole; sh, short hairpin.

Table S6. Correlation between BAP1 and PTEN in HCC

	BAP1-low	BAP1-high	Total
PTEN-low	125	47	172
PTEN-high	58	166	224
Total	183	213	396

P <0.001, $r = 0.465$.

BAP1 suppresses HCC invasion by deubiquitinating PTEN

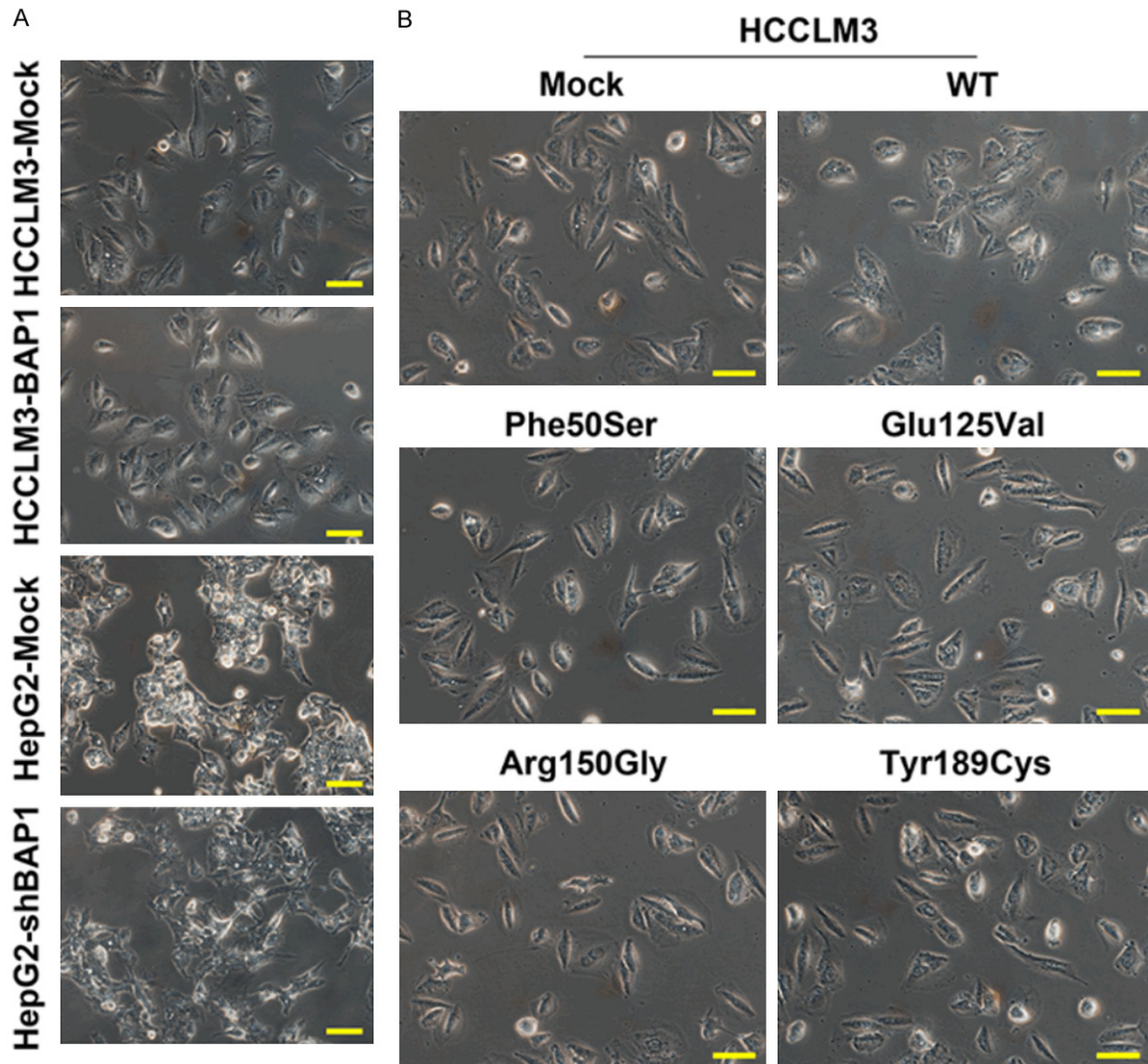


Figure S3. BAP1 deficiency induced HCC cell EMT. A. Representative images showing the morphology of indicated HCC cells. B. Representative images showing the morphology of indicated HCC cells. Scale bars = 100 μ m. Abbreviations: WT, wild type.

BAP1 suppresses HCC invasion by deubiquitinating PTEN

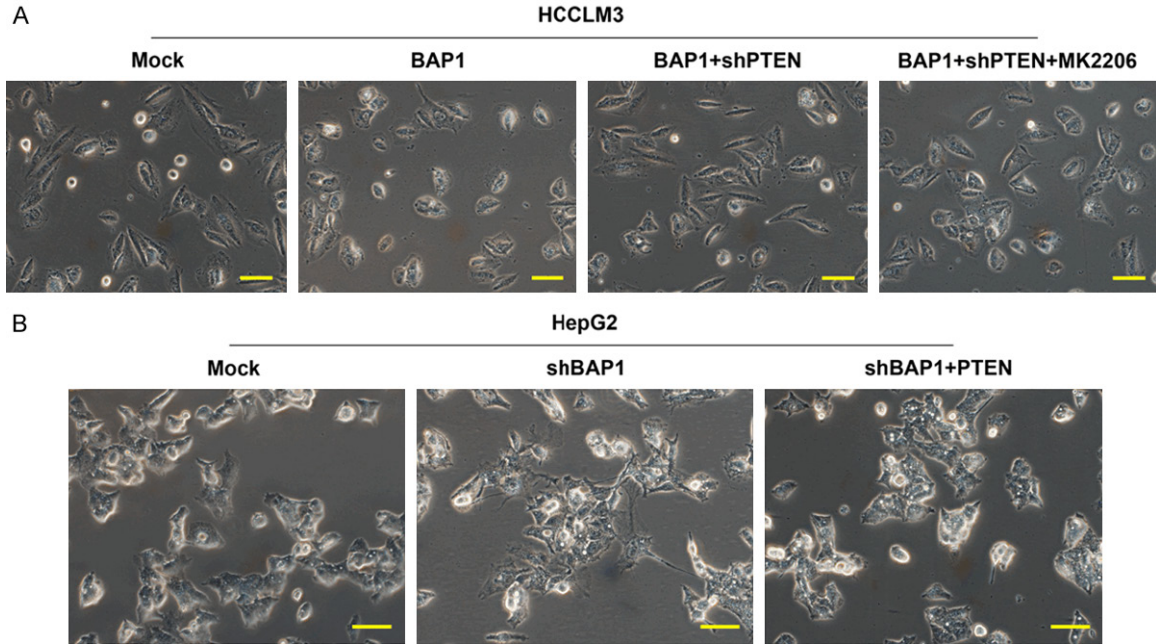


Figure S4. PTEN protein level is vital for BAP1-regulated HCC cell EMT. A. Representative images showing the morphology of indicated HCC cells. B. Representative images showing the morphology of indicated HCC cells. Scale bars = 100 μ m.

BAP1 suppresses HCC invasion by deubiquitinating PTEN

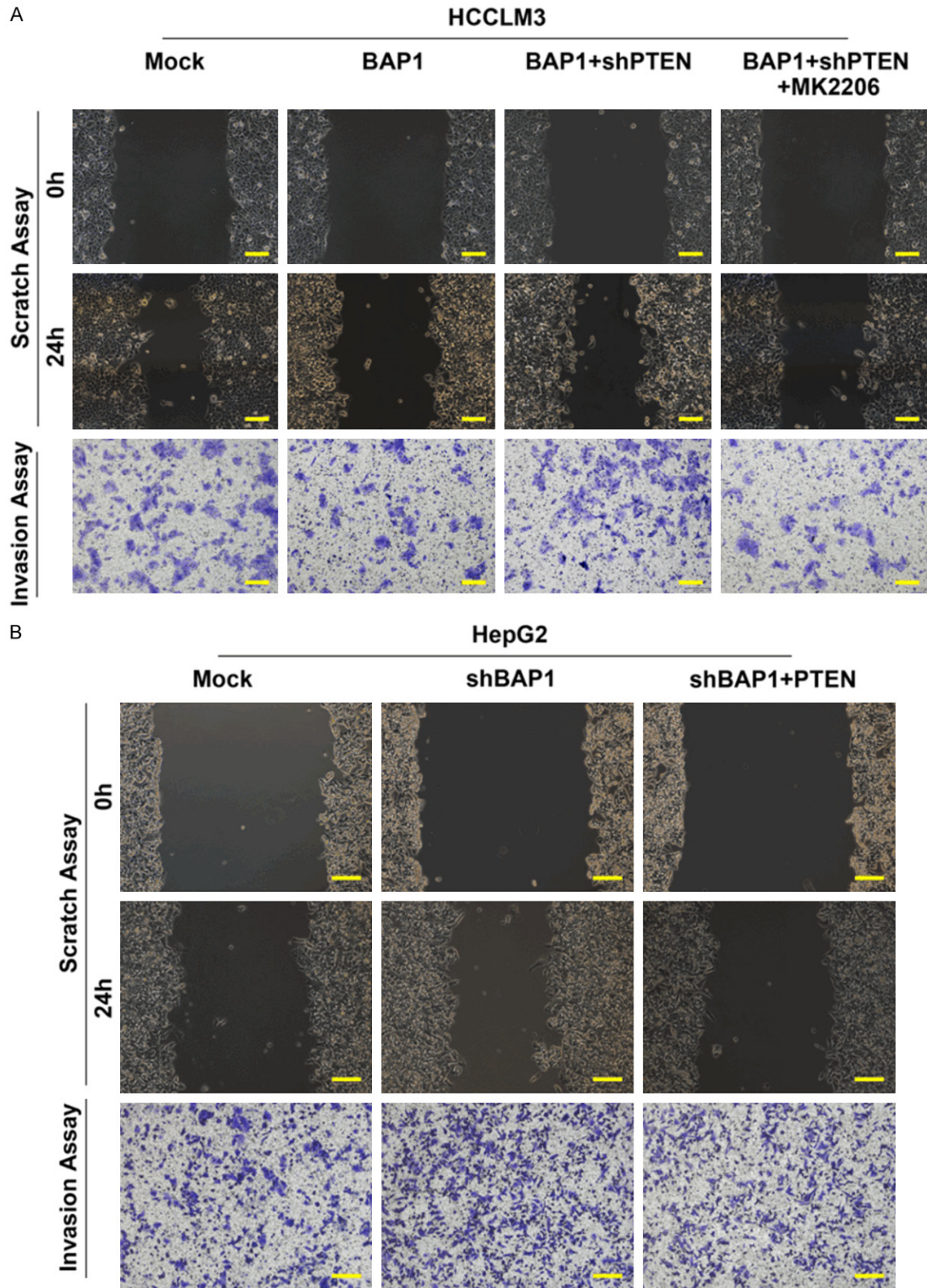


Figure S5. PTEN protein level is vital for BAP1-regulated HCC cell invasion. A. The migratory and invasive capacities of indicated HCCLM3 cells were examined by functional assays *in vitro*. B. The migratory and invasive capacities of indicated HepG2 cells were examined by functional assays *in vitro*. Scale bars = 200 μ m.